The application of MC codes in radiation physics and dosimetry

Lecture 3

Induced radioactivity, instrumentation and dosimetry

M. Silari, CERN

Outline

- Induced radioactivity in accelerators
  - Decommissioning of LEP
  - The “zoning” of ATLAS
  - Predicting doses in the LHC
- Design of monitoring instrumentation
  - Neutron monitors and spectrometers
  - Tissue equivalent proportional counters
- Accident dosimetry
- Radiation dosimetry for Hiroshima and Nagasaki

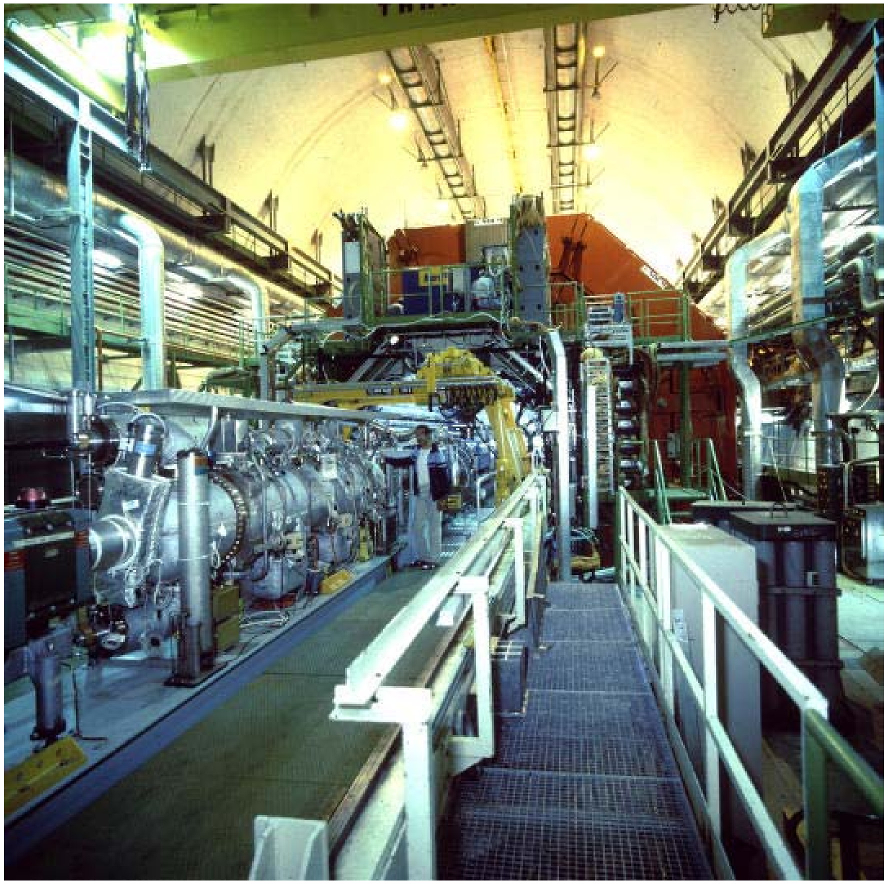

Do you remember LEP?
A little bit of history

- Start of operation: 1989
- 1989-95: 45 GeV
- October 1995: 68 GeV
- June 1996: 80.5 GeV
- October 1996: 86 GeV
- 1997: 92 GeV
- 1998: 94.5 GeV
- 1999: 100 GeV
- 2000: 104 GeV
- 2001: decommissioning

LEP was classified as Nuclear Basic Installation (*Installation Nucléaire de Base*, INB) in France, where no unconditional clearance levels exist for specific activity in materials to be released into the public domain.

Release of material may only be allowed if a detailed theoretical study – supported by experimental measurements – has shown which parts of the machine could (or could not) have been subjected to activation phenomena. -> 25,000 tons of equipment from the LEP machine areas and 10,000 tons from the experiments

For the *zoning* study 1/10 of the exemption limits as given by the European Directive (EU) of 13 May 1996 in any material were taken as a reference.
→ 1 Bq/g for most radionuclides

The *zoning study* of LEP

(M. Silari and L. Ulrici, NIMA 526 (2004) 510)

- 2 methods:
  - Monte-Carlo calculations
  - Experimental measurements (material samples exposed on beam dumps 1997-2000, dipoles)
- 4 possible activation phenomena:
  - localised beam losses (e.g., collimators), which were the predominant source in most parts of the ring
  - distributed beam losses (mainly at the beginning of the arcs)
  - synchrotron radiation for E > 100 GeV
  - high-energy X-rays emitted by the super-conducting RF cavities

Radioactivity induced by synchrotron radiation

Total specific activity (Bq/g) in various regions of the LEP dipoles induced by synchrotron radiation for a beam energy of 100 GeV predicted by FLUKA

Decay time (days)	Al (vacuum chamber)	Pb (shield)	Iron-concrete (dipole)
0	$3.38\ 10^{-1}$	$6.41\ 10^{-1}$	$3.56\ 10^{-2}$
1	$1.29\ 10^{-1}$	$4.53\ 10^{-1}$	$5.14\ 10^{-3}$
7	$3.64\ 10^{-2}$	$7.43\ 10^{-2}$	$3.75\ 10^{-3}$
30	$3.44\ 10^{-2}$	$4.36\ 10^{-3}$	$3.52\ 10^{-3}$
365	$1.76\ 10^{-2}$	$5.17\ 10^{-4}$	$1.96\ 10^{-3}$
3650	$4.30\ 10^{-4}$	$4.77\ 10^{-7}$	$9.96\ 10^{-5}$

G.R. Stevenson and A. Leuschner

Localized beam losses

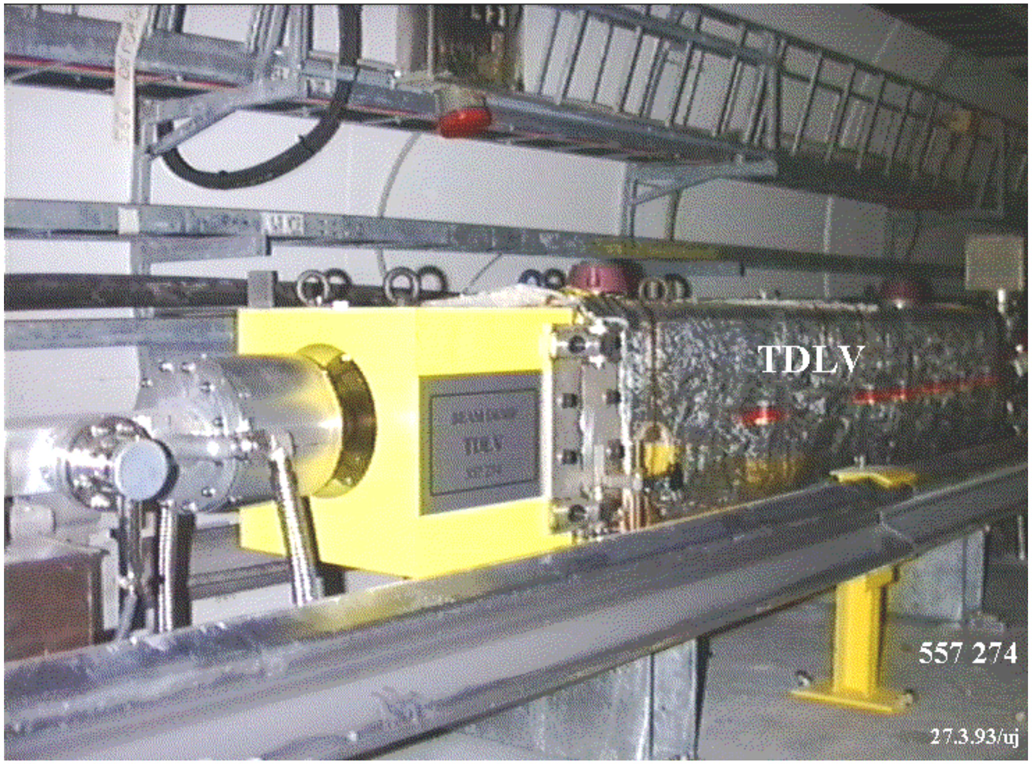

- Monte-Carlo (FLUKA): direct scoring of the radionuclide yield by the RESNUCLEI option
- Material samples were irradiated on both dumps for approximately five months in the years 1997-2000 and activated by the stray radiation; the results were normalized to the beam power deposited in the dump.

All radionuclides with a half-life longer than 60 days were predicted by FLUKA to within a factor of 2 of the experimental value, and several of them with even a better accuracy.

Induced radioactivity in accelerators

Radio-nuclide	$T_{1/2}$	Possible production reactions	A_S at saturation (Bq/g per watt)
$^{3}H^{(\#)}$	12.3 y	Spallation	$3.1\ 10^{-1}$
^{46}Sc	83.8 d	Spallation	$3.5\ 10^{-2}$
^{54}Mn	312.2 d	Spallation $^{55}Mn(\gamma,n)$	$6.8\ 10^{-1}$
^{56}Co	77.7 d	Spallation $^{56}Fe(p,n)$	$4.9\ 10^{-1}$
^{57}Co	271.8 d	$^{63}Cu(\gamma,2p4n)$ $^{56}Fe(p,\gamma)$ $^{57}Fe(p,n)$ $^{59}Co(\gamma,2n)$	2.2
^{58}Co	70.9 d	$^{63}Cu(\gamma,2p3n)$ $^{57}Fe(p,\gamma)$ $^{59}Co(\gamma,n)$	3.1
^{60}Co	5.27 y	$^{63}Cu(\gamma,2pn)$ $^{65}Cu(\gamma,2p3n)$ $^{59}Co(n,\gamma)$	2.8
^{65}Zn	244 d	$^{64}Zn(n,\gamma)$ $^{66}Zn(\gamma,n)$ $^{65}Cu(\gamma,pn)$	$3.6\ 10^{-2}$

Localized beam losses

Conversion coefficients from average beam power (watt) to induced specific radioactivity at saturation A_S (Bq/g) for radionuclides produced in copper. Part of the induced activity comes from impurities.

Radio-nuclide	A/A_S	Induced specific activity (Bq/g per watt)				
		Al	Cu	St.-steel	Iron-conc.	Pb
^{3}H	0.218	0.72	0.07	0.08	0.39	0.06
^{22}Na	0.496	1.09	–	0.05	0.15	–
^{46}Sc	0.816	–	0.03	0.32	0.11	–
^{54}Mn	0.600	0.19	0.41	6.2	3.7	–
^{56}Co	0.833	–	0.41	1.2	0.12	0.03
^{57}Co	0.614	–	1.35	5.1	0.001	–
^{58}Co	0.853	–	2.6	6.6	0.005	0.001
^{60}Co	0.378	–	0.87	0.20	–	–
^{65}Zn	0.627	–	0.02	–	0.002	–
^{85}Sr	0.874	–	–	0.26	–	–
^{88}Y	0.762	–	–	0.03	–	0.001
^{88}Zr	0.817	–	–	0.03	–	0.007
^{110}Ag	0.622	–	–	–	–	0.002
^{124}Sb	0.889	–	–	–	–	2.8
^{207}Bi	0.097	–	–	–	–	0.13

Localized beam losses

- Typical scenario:
  - 1 W of beam power lost on a component
  - 10 years LEP lifetime with 6 months operation followed by 6 months shutdown.

↓

Estimated induced specific activity in LEP materials around a loss point (e.g., a collimator).

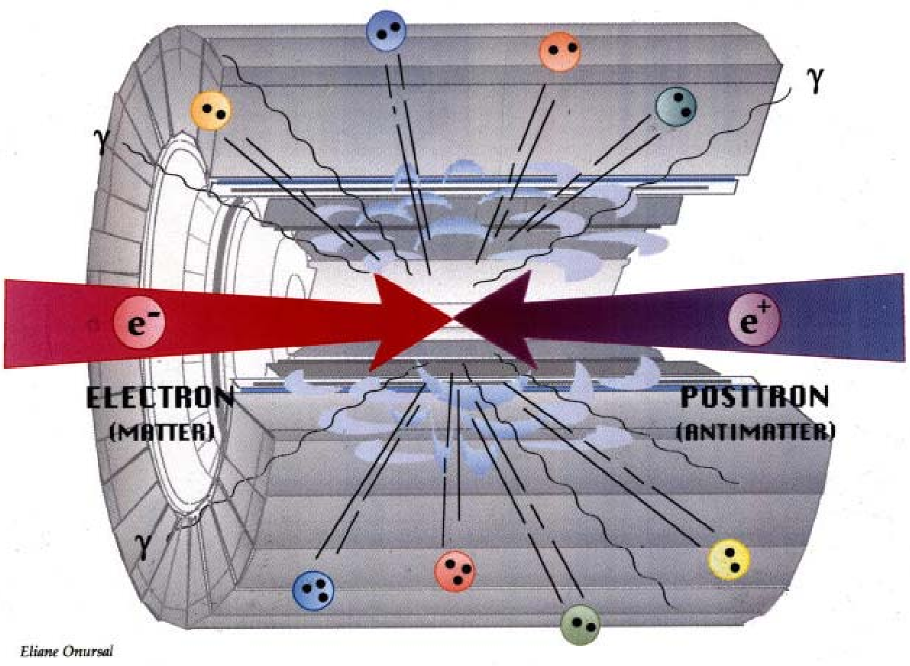

Simplified but conservative approach adopted for the zoning of the experiments

- adoption of a simplified, common geometry, for the calculations
- assumptions on the potential sources of induced activity
- Monte Carlo simulations
- experimental measurements

Calculations:

1) activation of the bulk of the detector by the hadronic components from $e^+ e^-$ events, and 2) activation of some of the forward and far-forward monitors by off-energy electrons from LEP as well as hadrons from two-photon interactions.

So far for LEP... now comes the LHC (and things get more complicated)

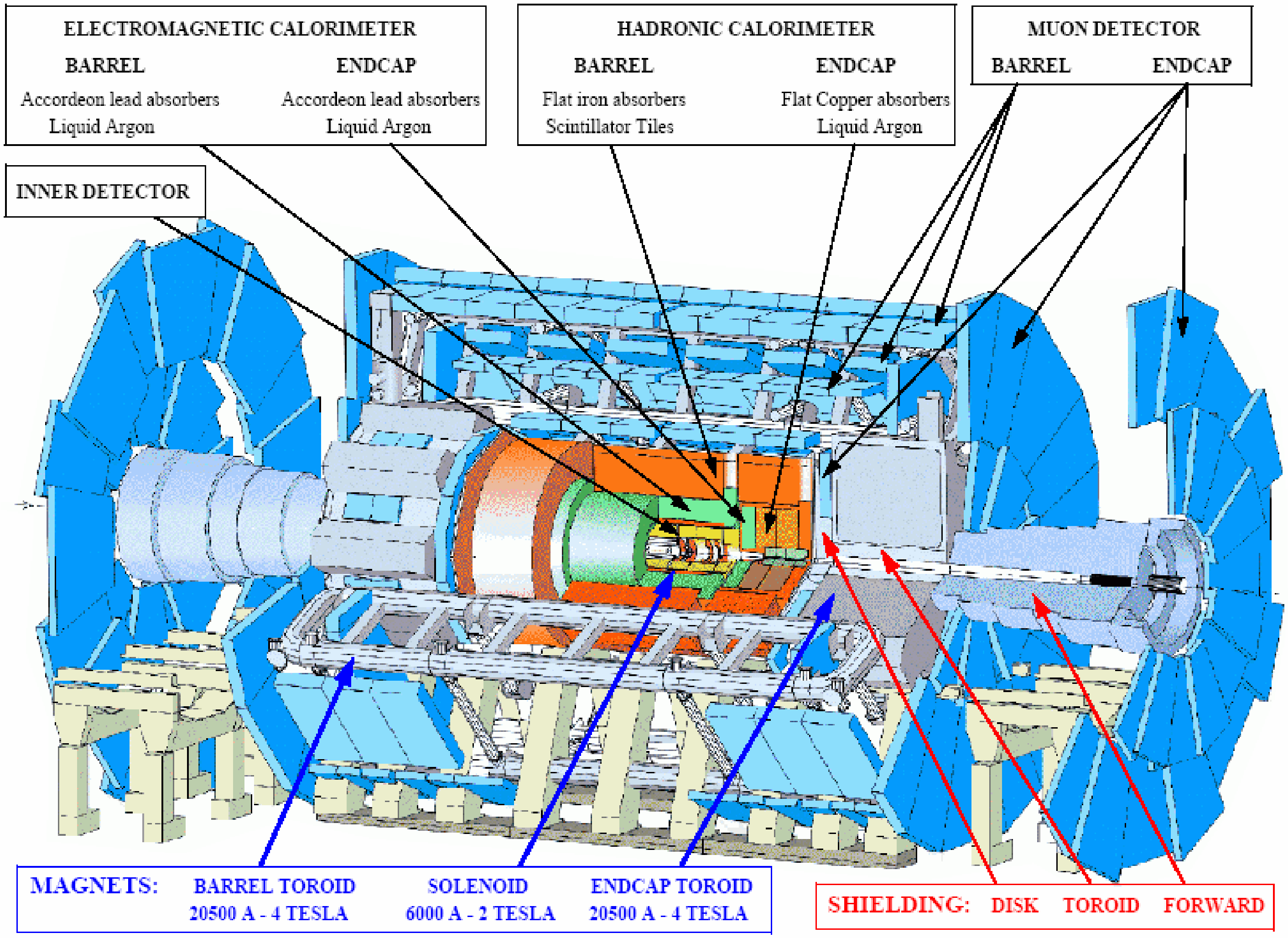

FLUKA calculations for the ATLAS zoning study

(M. Magistris and Z. Zajacova)

- Approach A
  - offline generator of p-p collisions
  - production rate of radioisotopes per region and per p-p collision with RESNUCLEI, followed by an offline treatment of the results for the build-up and decay of radioactivity and the normalization of the results to the radionuclide-specific exemption limits
  - the method was applied to 157 out of the 810 regions constituting the ATLAS geometry
  - the result is the number of radioactive isotopes per region normalized to one p-p collision event
  - successive decays included until the third generation
  - to calculate the specific activity per region, the region volumes had to be calculated. A special Monte Carlo technique was developed for this purpose

- Approach B
  - online treatment of the production and time evolution of residual nuclei, which considers all possible successive decays down to the last stable decay product
  - normalization of the results with the exemption limits in an online weighting routine
  - the results provided by the simulation are given as

$$\sum_i \frac{A_i}{LE_i}$$

  - the results for individual radioisotopes (specific activity, mass and atomic number) are lost in the simulation process
  - scoring on a region-independent RZ geometrical mesh encompassing the whole detector, with individual bins 5 cm in Z, 5 cm in R and extending over the full azimuthal angle
  - the detector being almost symmetric around its axis, a precise spatial distribution of activity can be obtained and, at the same time, bins are large enough to provide good statistics

Nuclear waste zoning of ATLAS that cuts through major items

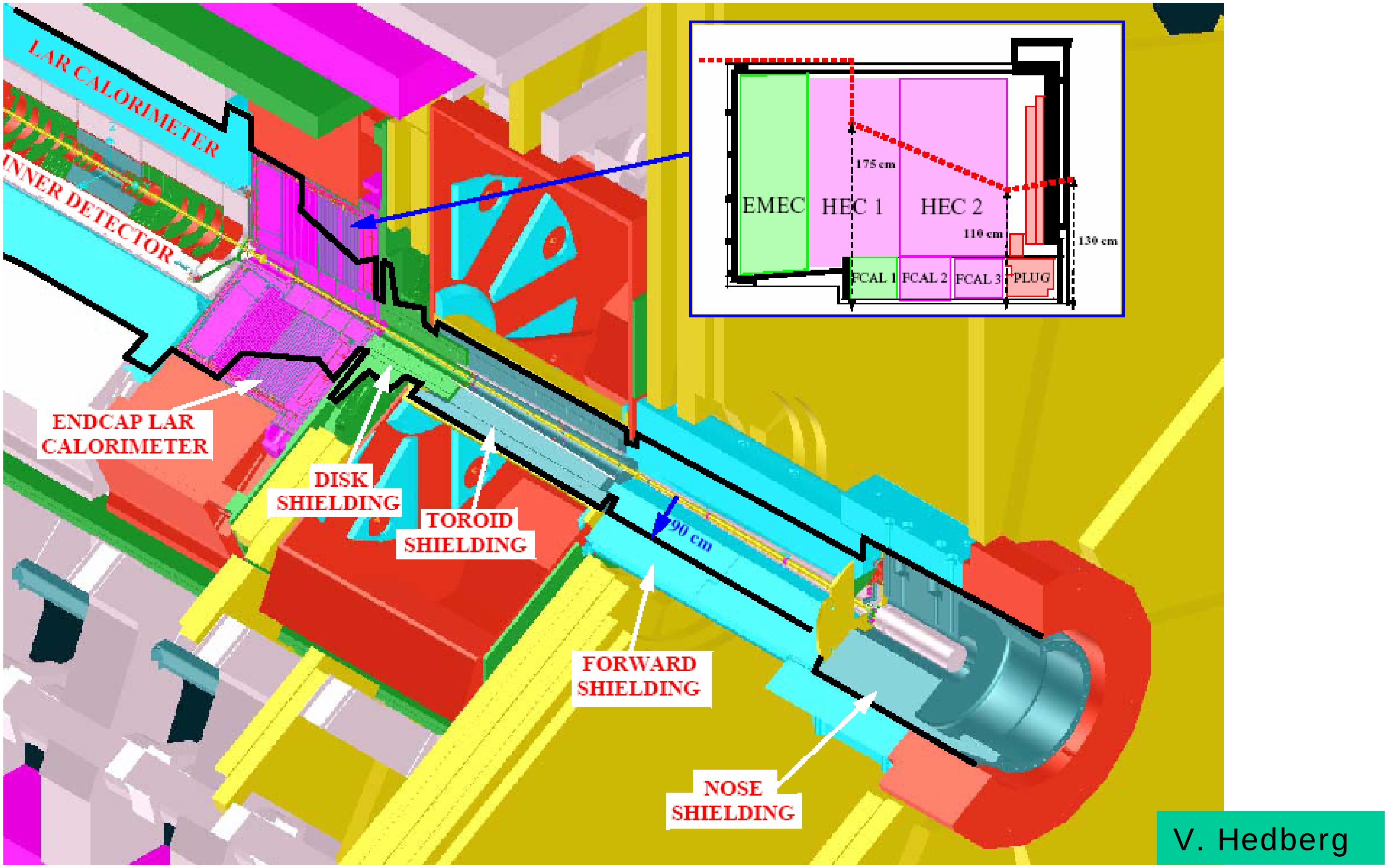

http://atlas.web.cern.ch/Atlas/TCOORD/Activities/CommonSys/Shielding/Activation/act_zoning.html

LHC Collimation

(M. Brugger, D. Forkel-Wirth, S. Roesler)

- LHC collimation system:
  - two cleaning insertions: Point 3 and Point 7
  - two- or three-stage collimation system with low-*Z* collimators (Carbon Composite Materials)
  - annual number of intercepted protons: ~10^{16}

The collimators will become one of the most radioactive component of LHC machine

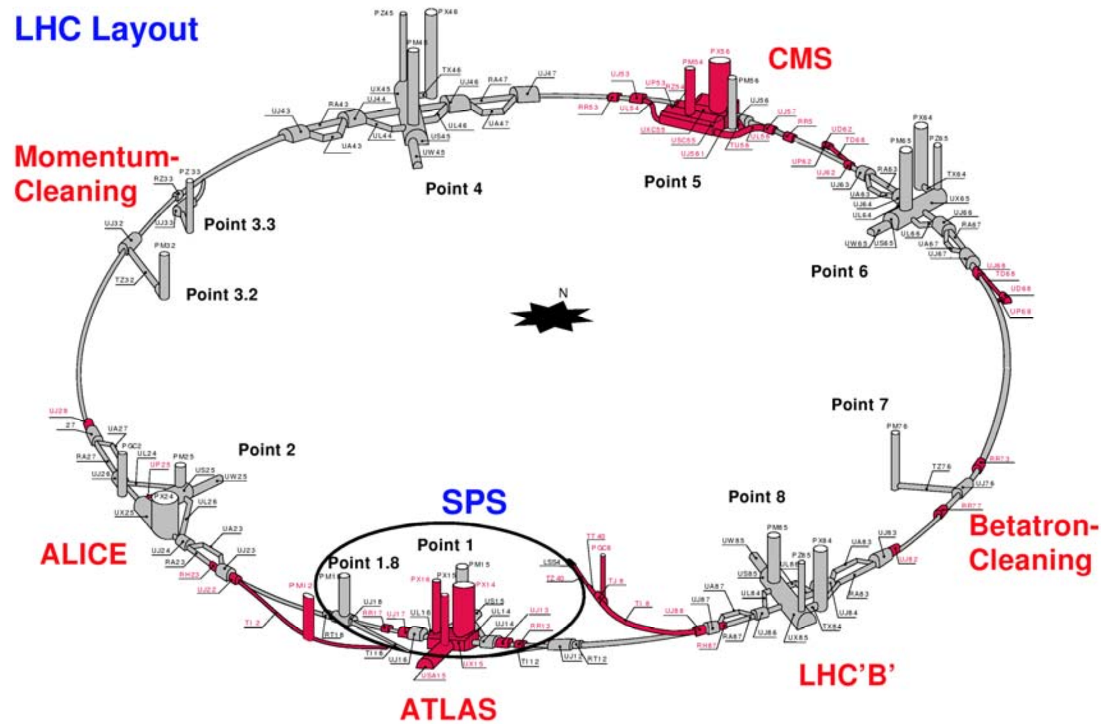

- Activation and remnant dose rate estimates are important criteria already in design phase of LHC
- Both installations are extraction points for the ventilation system, thus the release of radioactive air has to be studied in detail

1. Monte Carlo simulation (FLUKA, MARS) of particle interaction and transport in beamline and shielding components, tunnel / cavern air and walls.

Calculation of

inelastic interaction rate (without explicit isotope production)

isotope production rate

NEW

2. Calculation of remanent dose rates D_γ by using:

ω-factor approach

Assumption: contact dose rate is proportional to the density of inelastic interactions (*stars*)

$$\dot{D}_\gamma = \omega \times \rho_{star}$$

Advantages: allows fast estimates

Disadvantages:
- limited to contact dose rates from large objects
- typically given for 30d irrad. and 1d cooling

explicit Monte Carlo simulation of interactions and transport of radioactive decay products

Advantages:
- allows to calculate 3D dose rate maps for arbitrary geometries and irradiation histories
- most reliable method

Disadvantages: more time-consuming than ω-factor approach

LHC collimation region

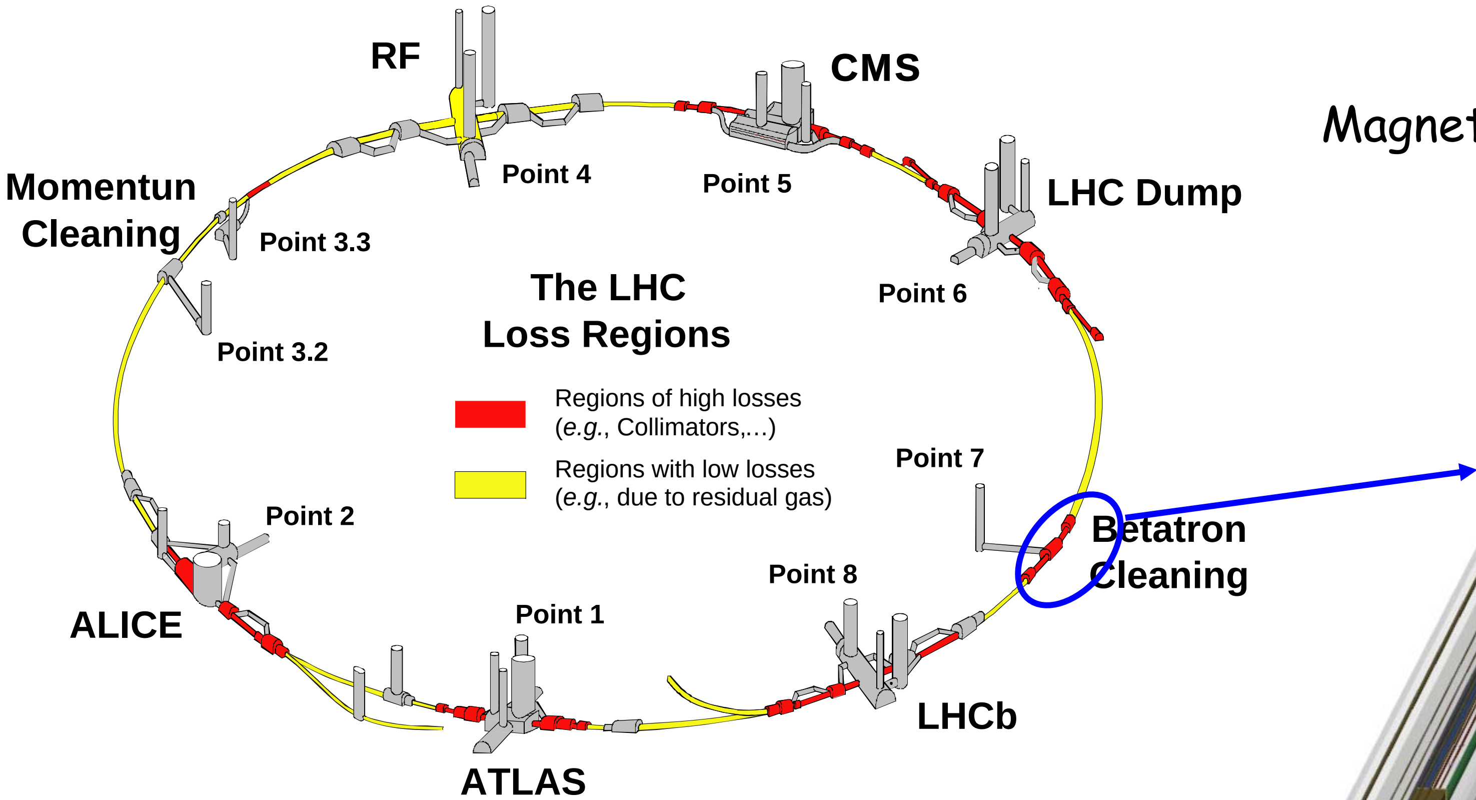

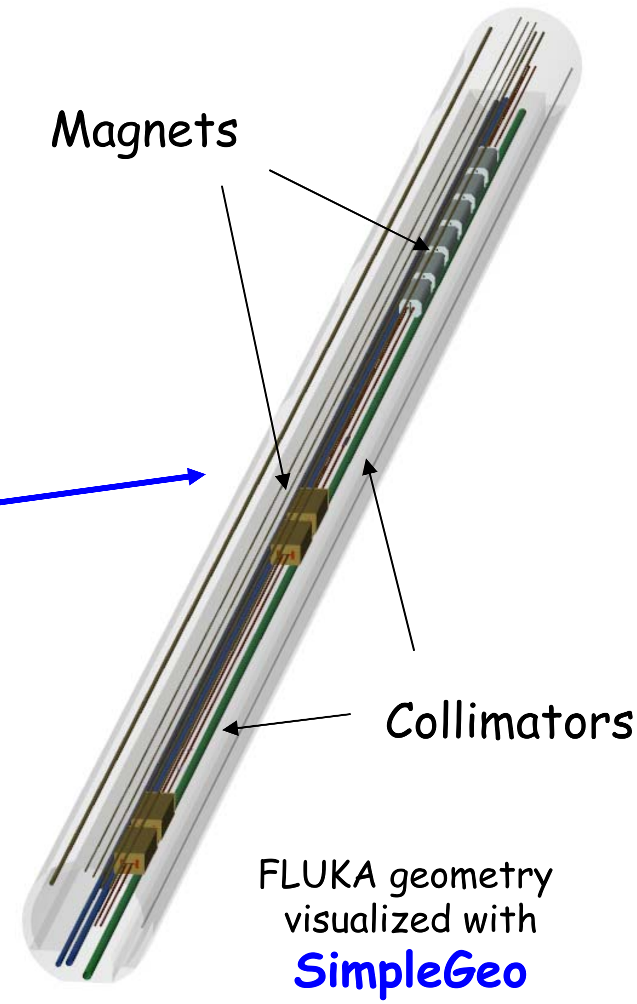

Courtesy A. Ferrari

Cooling time

8 hours

1 week

4 months

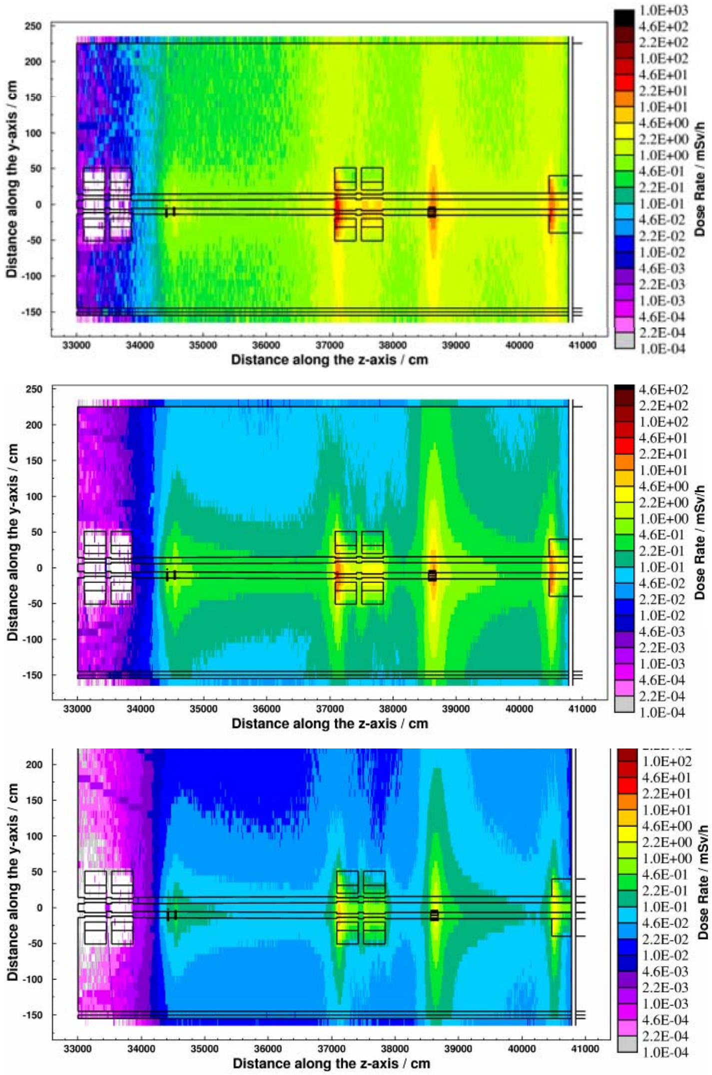

LHC collimation region

Residual dose rate (mSv/h) after one year of operation

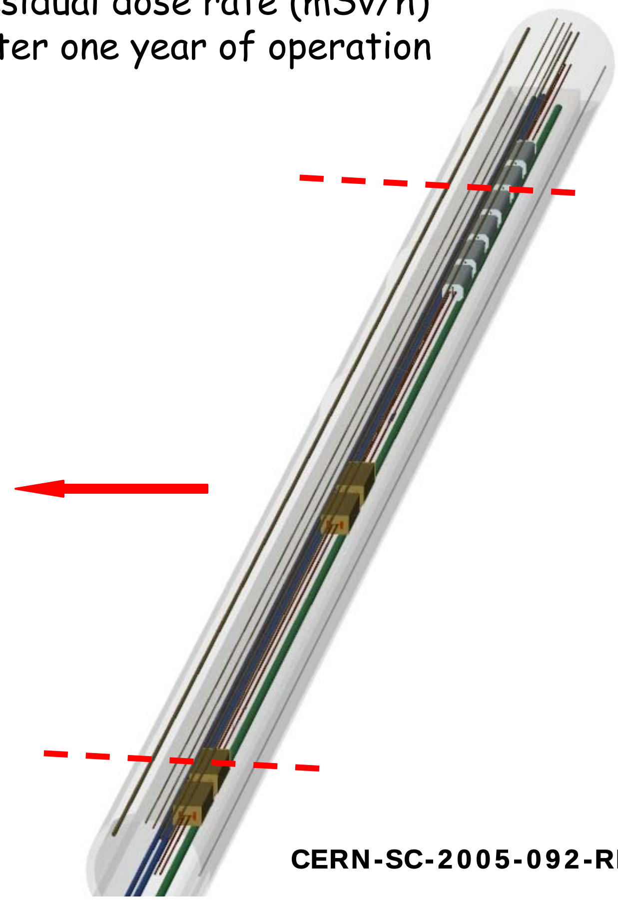

CERN-SC-2005-092-RP-TN

REMANENT DOSE RATE MAPS OF THE LHC BETATRON CLEANING INSERTION (IR7)

M. Brugger, D. Forkel-Wirth, S. Roesler

Exploded view of the original SNOOPY-modified rem counter → Long Interval NeUtron Survey-meter, LINUS

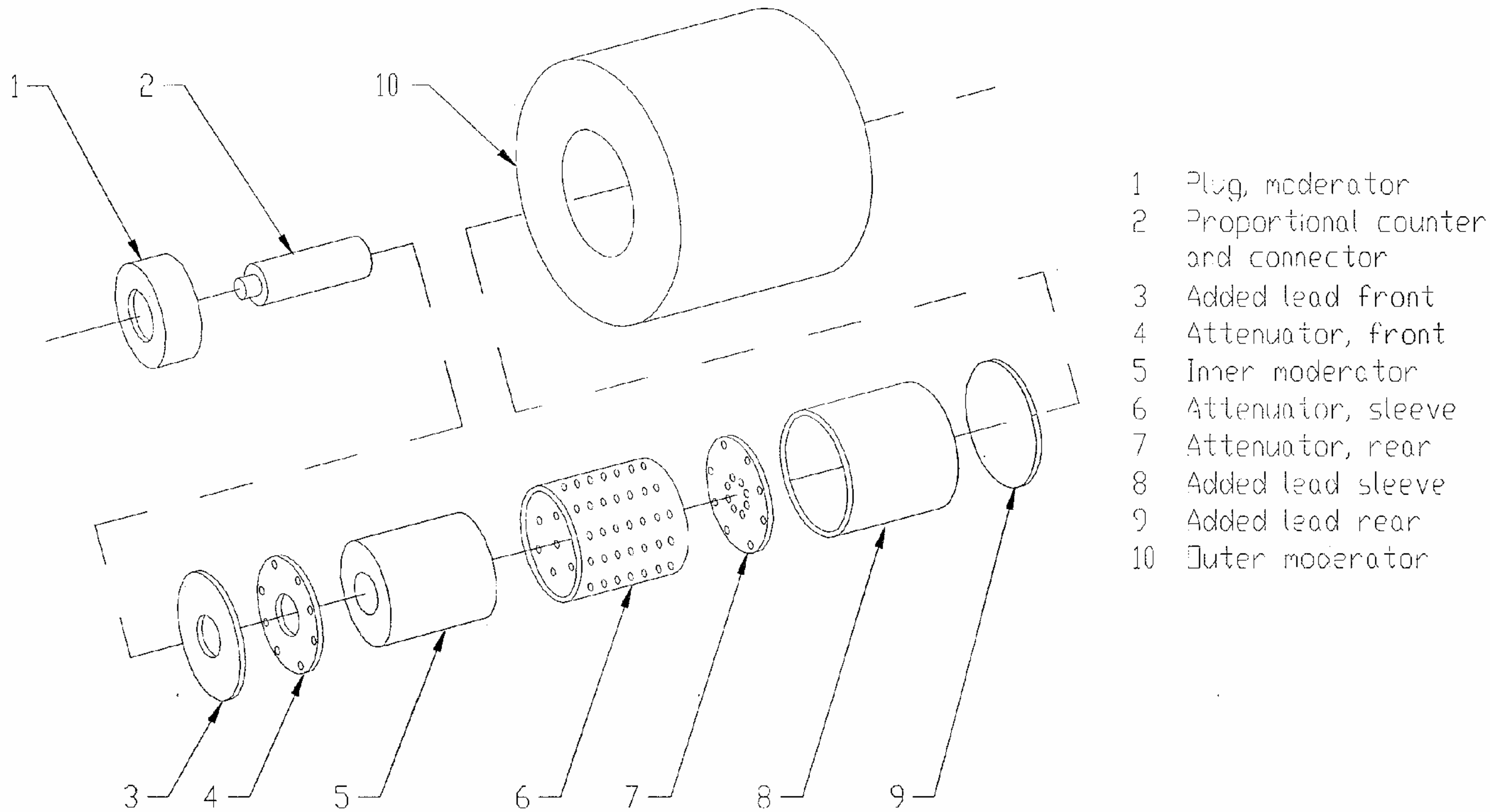

C. Birattari, A. Ferrari, C. Nuccetelli, M. Pelliccioni, M. Silari, NIMA 297 (1990) 250-257

Spherical LINUS

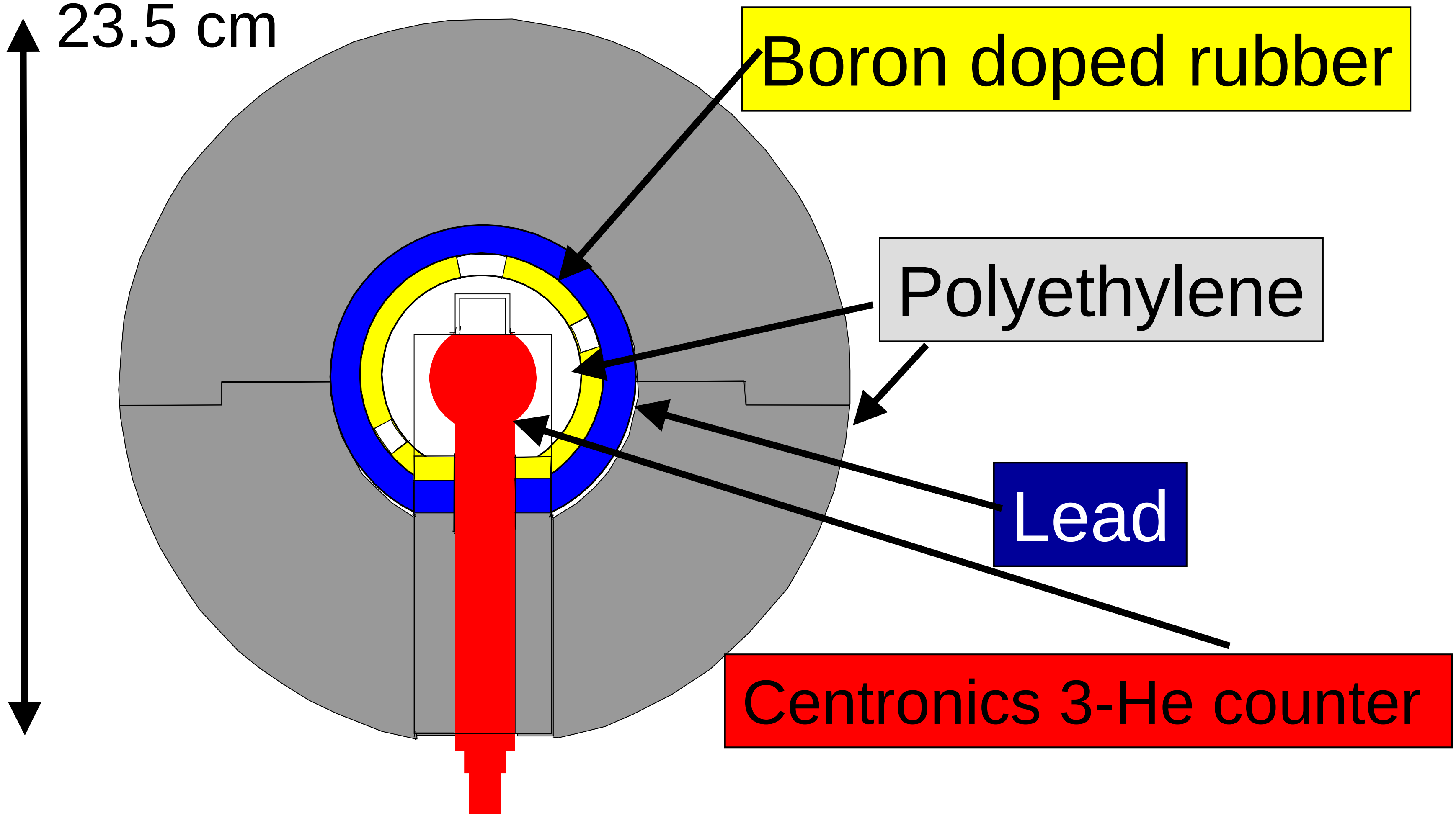

Absolute neutron fluence response

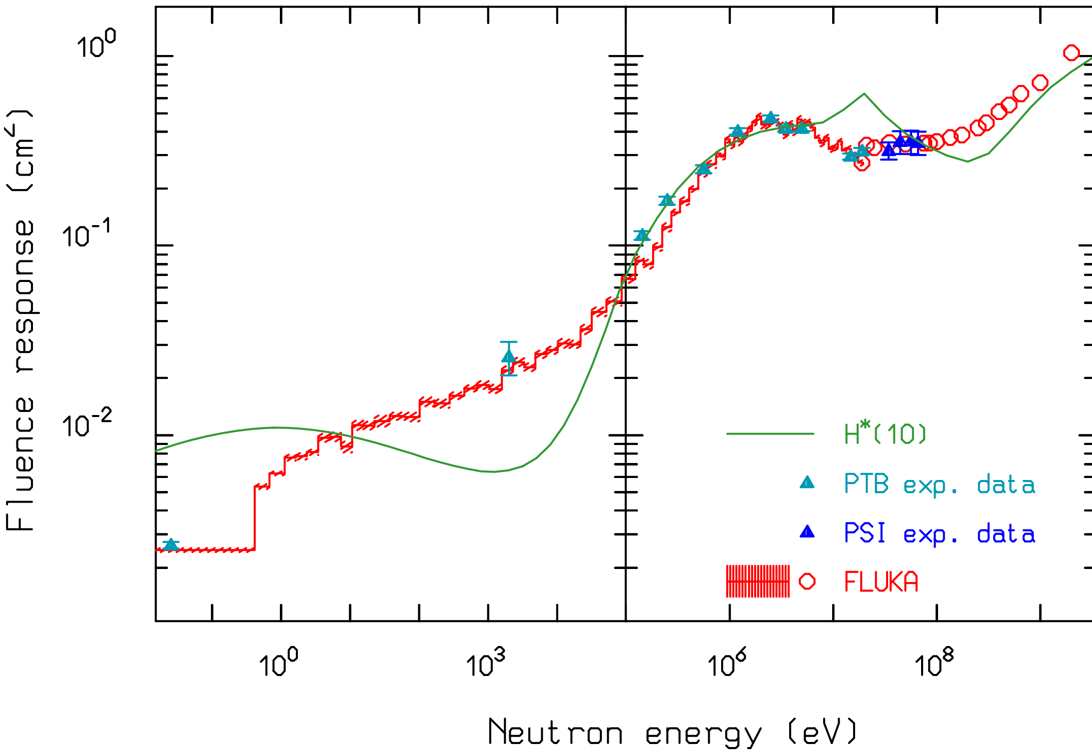

$$M = C\int R_{\Phi}(E)\,\Phi(E)\,dE$$

LINUS

SNOOPY

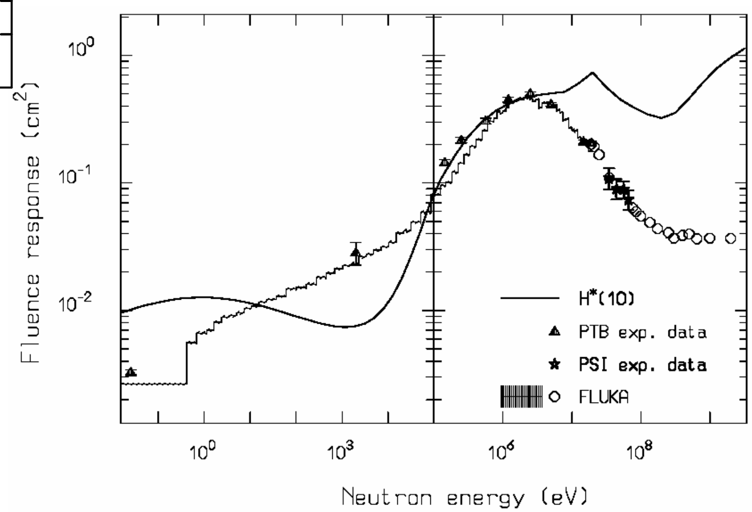

Calibration of the LINUS rem counter with monoenergetic neutron beams at PTB and with quasi-monoenergetic neutron beams at PSI (full symbols), compared with simulation (dashed histograms and open symbols)

Comparison of the response of rem counters in high-energy stray neutron field

Detector	Calibration		Ambient dose equivalent	
	Factor (nSv/cts)	Procedure	(nSv/PIC)	Total uncertainty
Studsvik (CERN)	0.98	H*(10), PuBe source	0.145	$1.64x10^{-2}$
Berthold (CERN)	0.353	H*(10), PuBe source	0.148	$1.49x10^{-2}$
Cylindrical LINUS (CERN)	1.49	H*(10), PuBe source	0.262	$2.95x10^{-2}$
Spherical LINUS (CERN)	0.92	H*(10), PuBe source	0.243	$2.77x10^{-2}$
Spherical LINUS (Univ. Mi)	0.776	H*(10), AmBe source	0.228	$2.49x10^{-2}$
Cylindrical LINUS (NRPB)	1.11	H*(10), AmBe source	0.247	$2.5x10^{-2}$
TEPC ICRP21			0.242	$3.0x10^{-2}$
TEPC CRP60			0.273	$2.7x10^{-2}$

Commercial versions of the LINUS

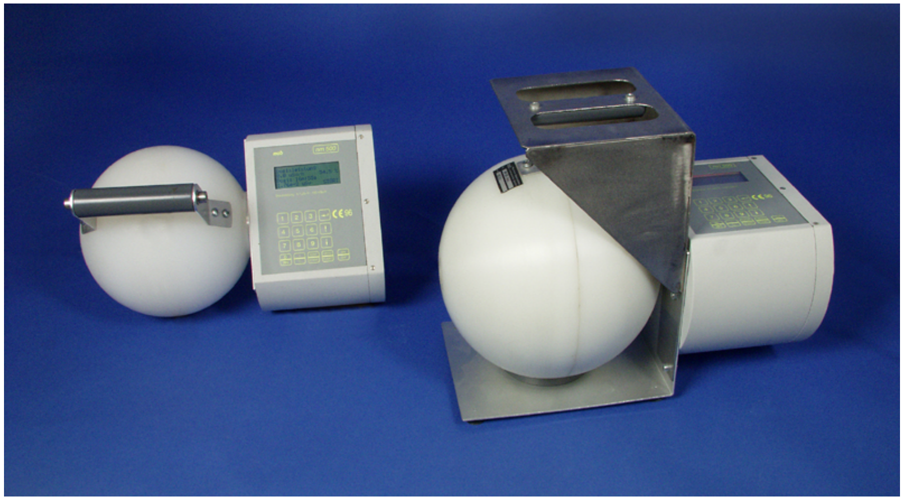

Spherical MAB Monitor SNM500(X)

WENDI II Monitor Eberline

Superheated emulsions (bubble detectors)

- Superheated liquid suspended in a gel
- The superheated droplets consisting of an over-expanded halocarbon and/or hydrocarbon which vaporizes upon exposure to the high-LET recoils from neutron interactions (a sort of miniature bubble chamber)
- Used as personal dosimeters, environmental dosimeters or spectrometers
- Insensitive to pulsed nature of radiation
- Insensitive to low-LET radiation

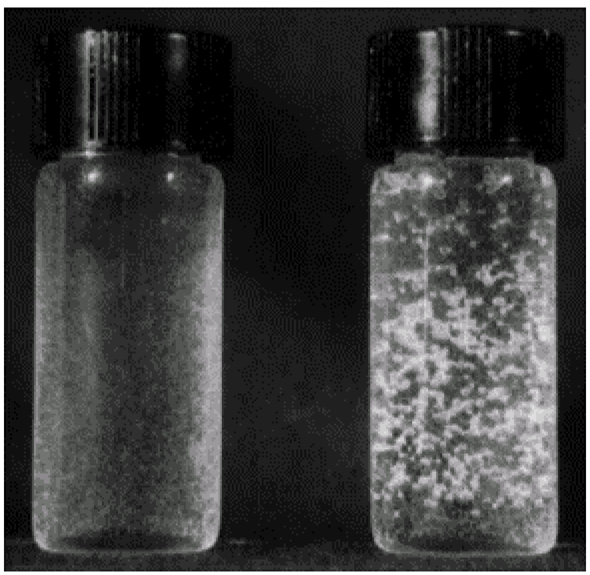

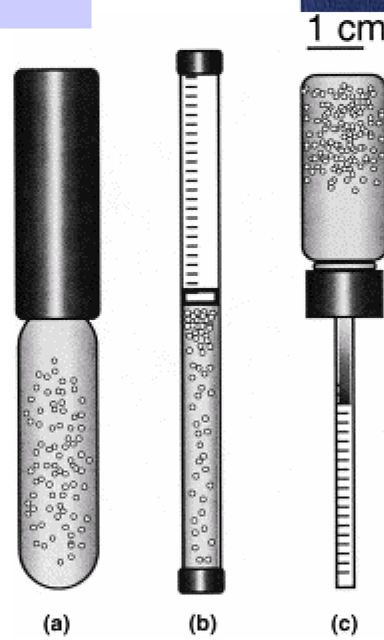

Neutron spectral fluence inside lead converters for the source neutrons on the CERF concrete roof-shield

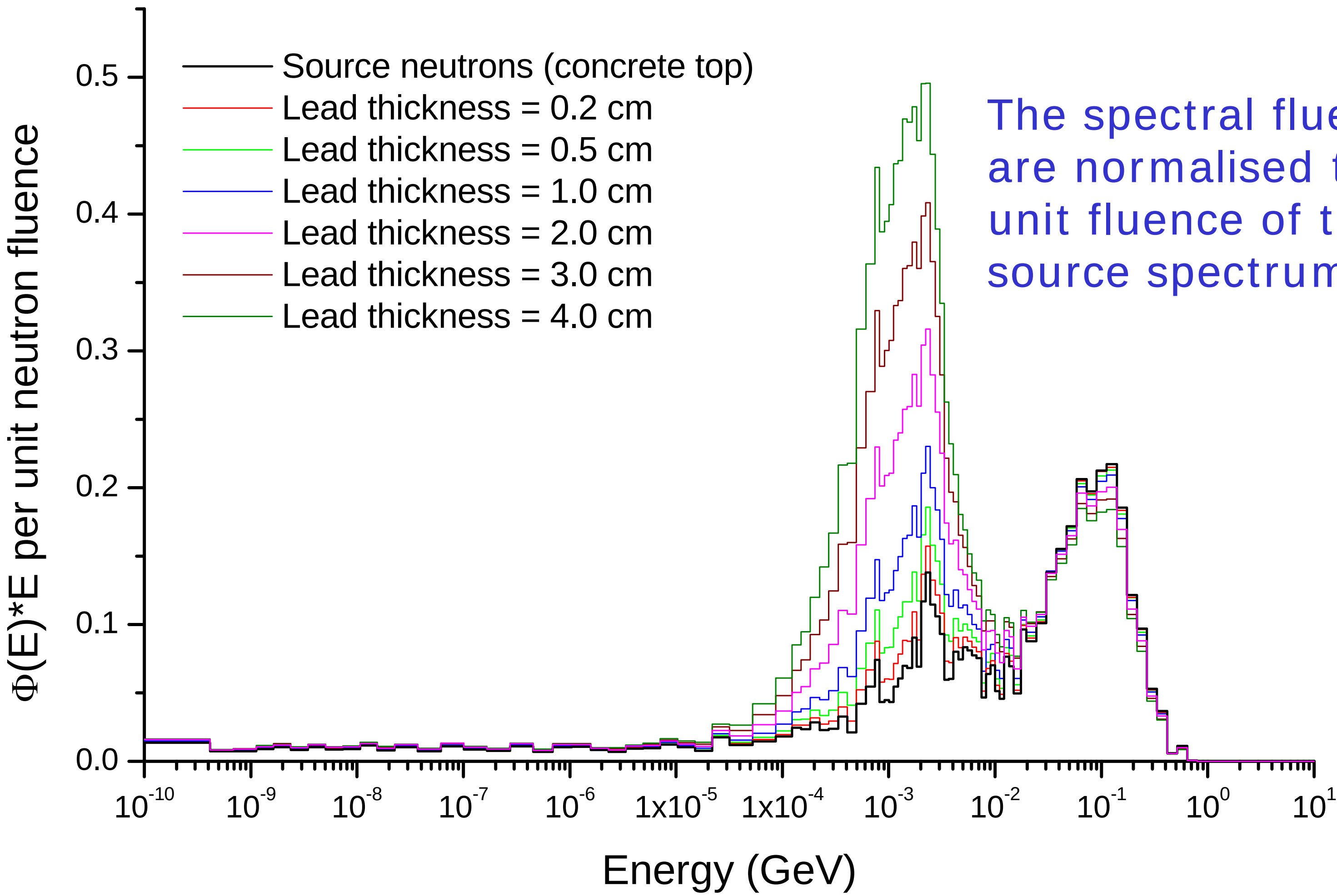

The spectral fluences are normalised to unit fluence of the source spectrum

Comparison experiment/Monte Carlo for the CERF concrete roof-shield

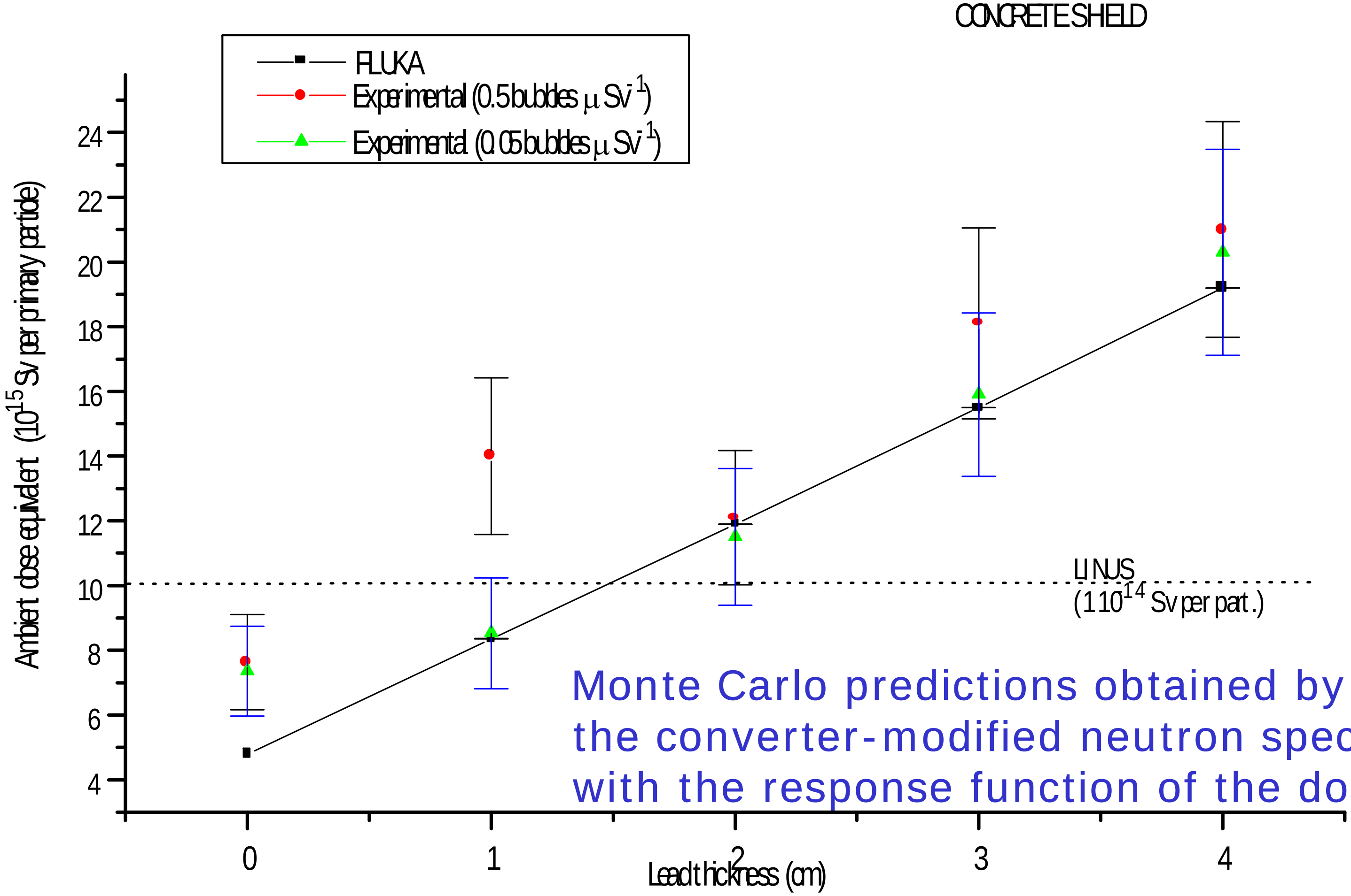

Monte Carlo predictions obtained by folding the converter-modified neutron spectrum with the response function of the dosemeter

S. Agosteo, M. Silari and L. Ulrici, Radiat. Prot. Dosim. 88, 149-155, 2000.

Acoustical bubble counters, open and with lead shell (F. d’Errico, University of Pisa)

Bonner Sphere Spectrometer (BSS)

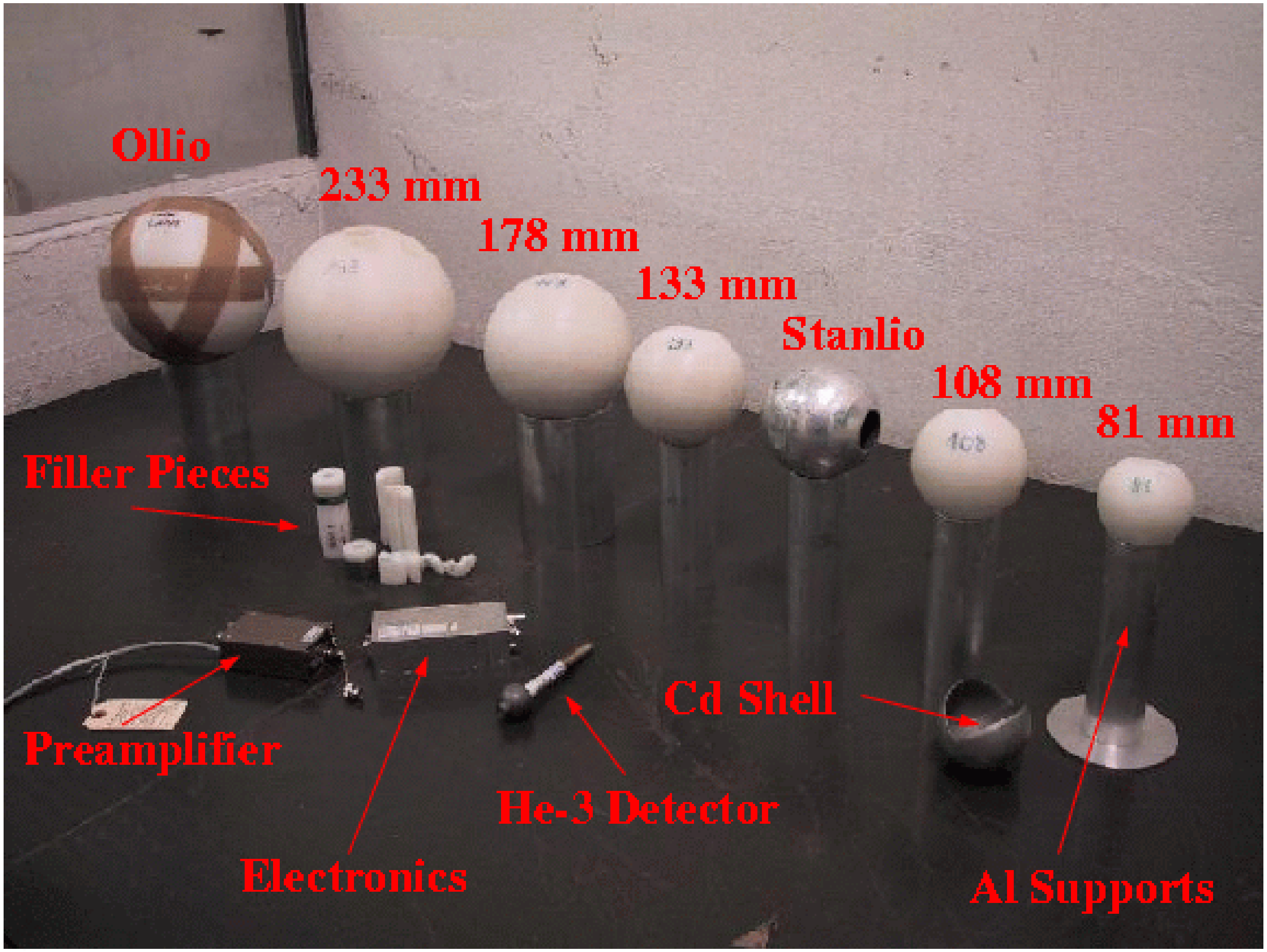

The BSS high-energy detectors

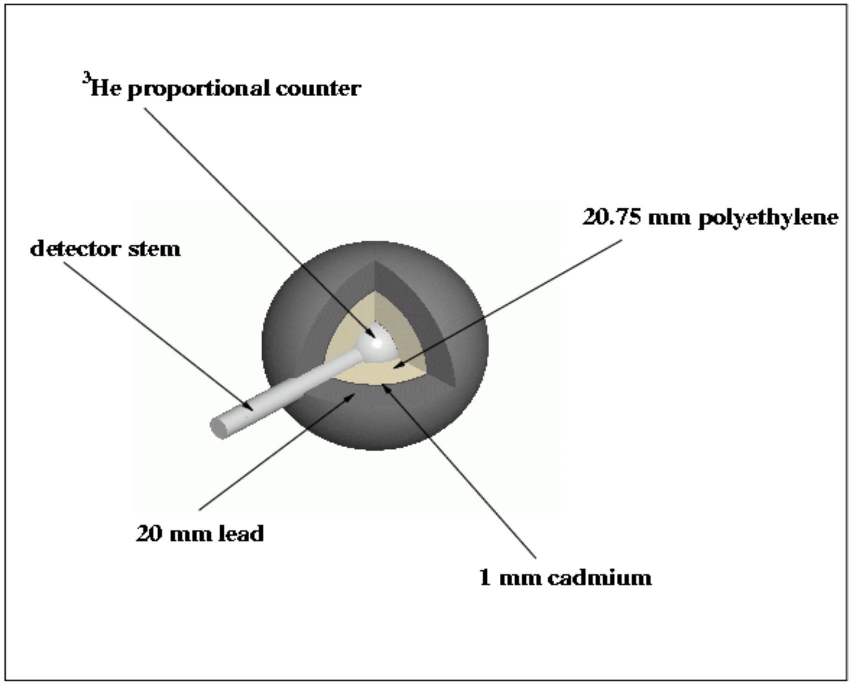

Stanlio

Ollio

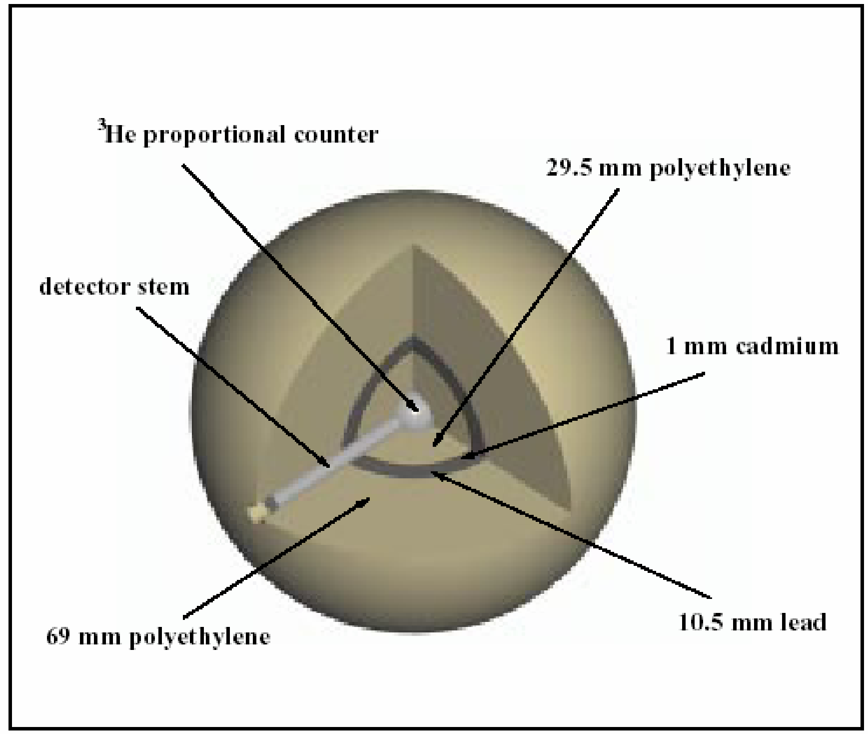

A. Mitaroff, PhD thesis (CERN and University of Vienna)

E. Dimovasili, PhD thesis (CERN and EPFL Lausanne)

C. Birattari et al, Proc. of Monte Carlo 2000, Lisbon, October 2000.

Absolute neutron fluence response functions of the BSS

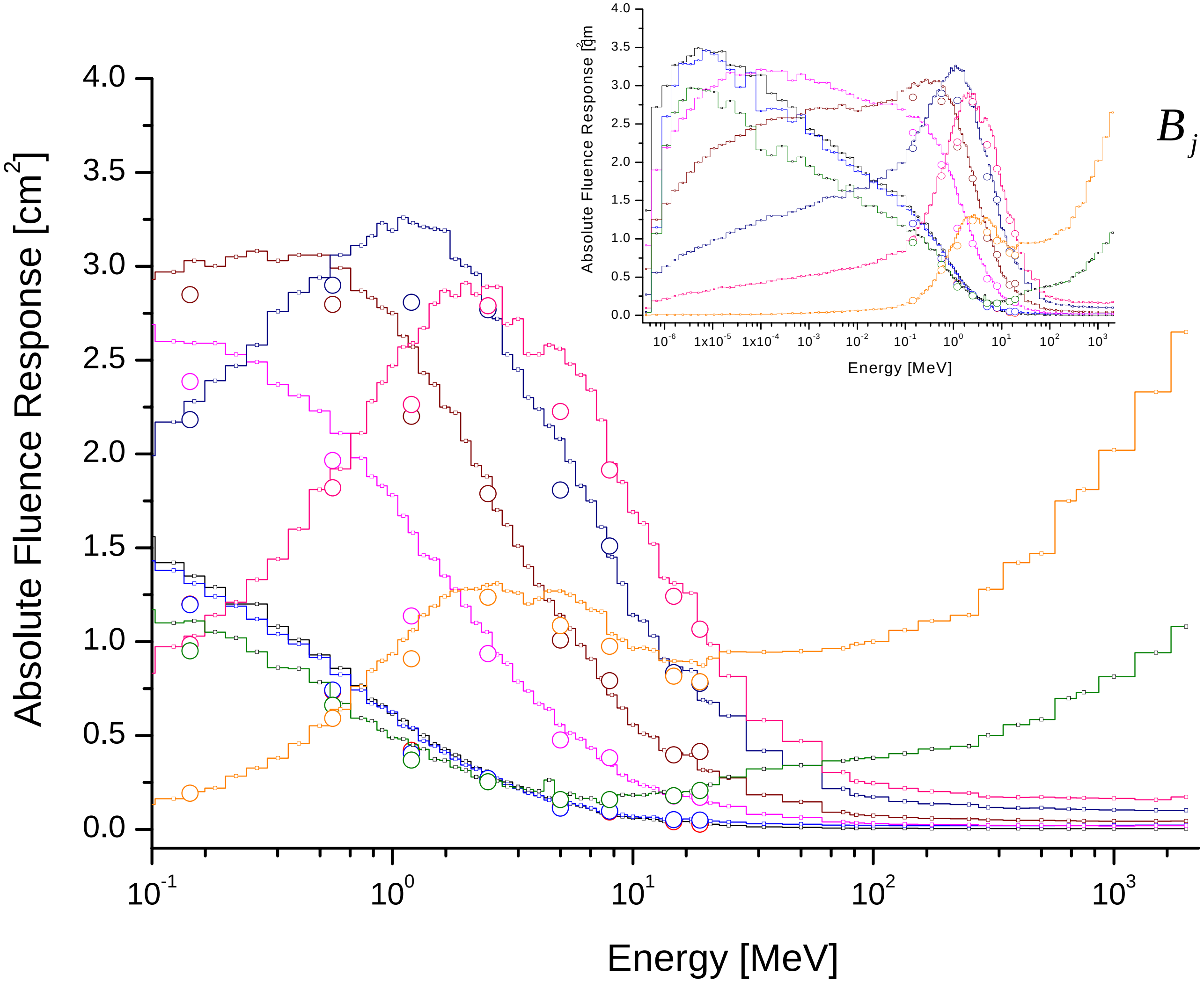

$$B_j = \int_0^\infty N(E) R_j(E) dE$$

Experimental and MC calculated absolute response of the extended BSS on the CERF concrete roof-shield

Sphere	**Response** (counts per incident hadron on the copper target)		
	Experimental	**Calculated**	**Ratio (calc/exp)**
83 mm + cadmium	$(1.38+/-0.07)x10^{-5}$	$(1.56+/-0.26)x10^{-5}$	1.13+/-0.19
83 mm	$(2.01+/-0.09)x10^{-5}$	$(2.30+/-0.31)x10^{-5}$	1.14+/-0.16
108 mm	$(2.72+/-0.12)x10^{-5}$	$(2.87+/-0.42)x10^{-5}$	1.06+/-0.16
133 mm	$(3.19+/-0.15)x10^{-5}$	$(3.20+/-0.47)x10^{-5}$	1.00+/-0.15
178 mm	$(3.23+/-0.15)x10^{-5}$	$(3.30+/-0.47)x10^{-5}$	1.02+/-0.15
233 mm	$(2.81+/-0.13)x10^{-5}$	$(2.96+/-0.40)x10^{-5}$	1.05+/-0.15
Stanlio	$(1.58+/-0.07)x10^{-5}$	$(1.93+/-0.29)x10^{-5}$	1.22+/-0.20
Ollio	$(1.93+/-0.09)x10^{-5}$	$(2.36+/-0.32)x10^{-5}$	1.22+/-0.17

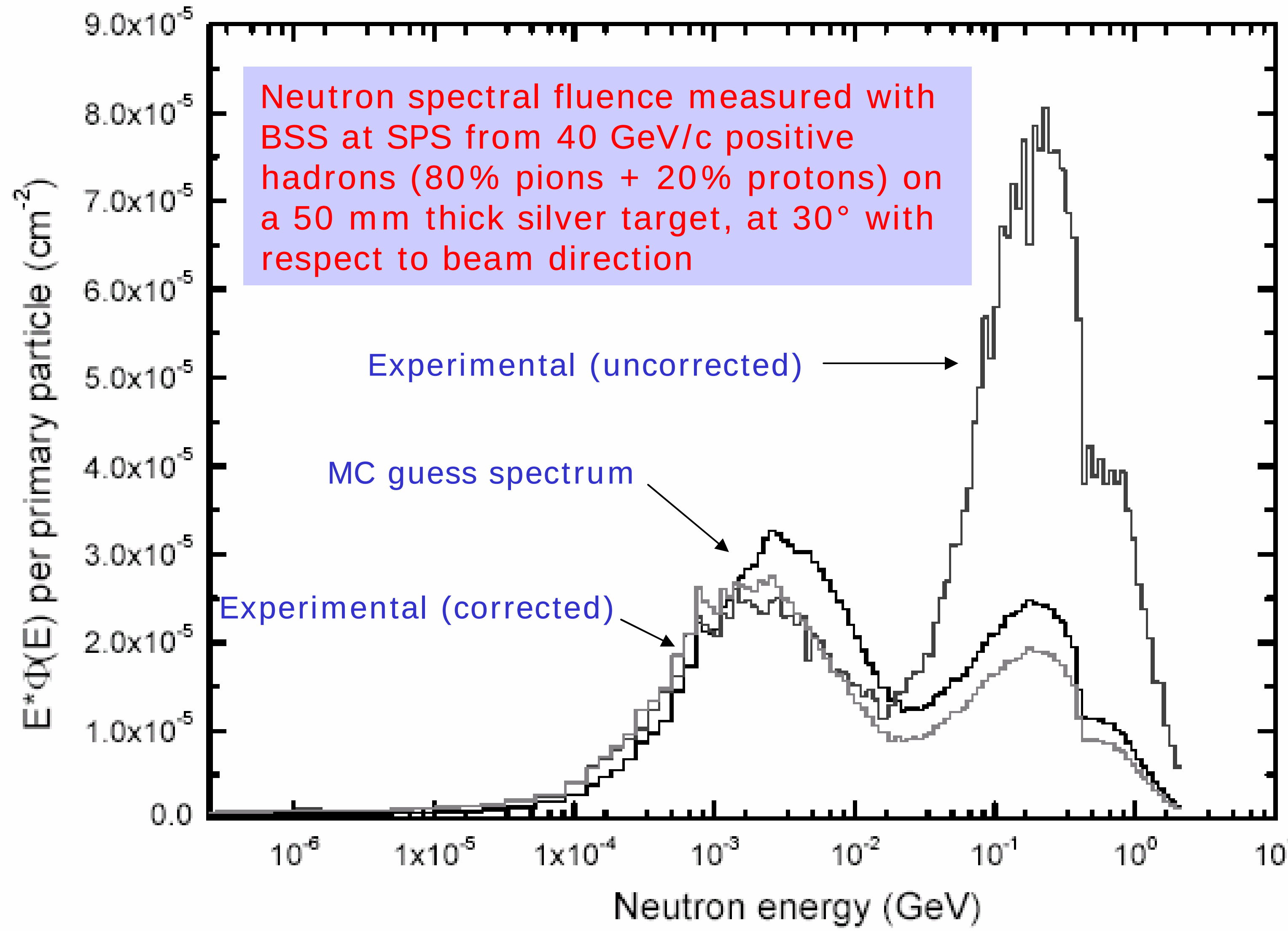

S. Agosteo, E. Dimovasili, A. Fassò and M. Silari, Radiat. Prot. Dosim. 110, 161-168, 2004

Spectral fluences of neutrons and charged hadrons at 30° from 40 GeV/c positive pions striking a 50 mm thick silver target, calculated by Monte Carlo

Correction factor =

$$\frac{\text{(contribution of neutrons)}}{\text{(Sum of contributions of all particles)}}$$

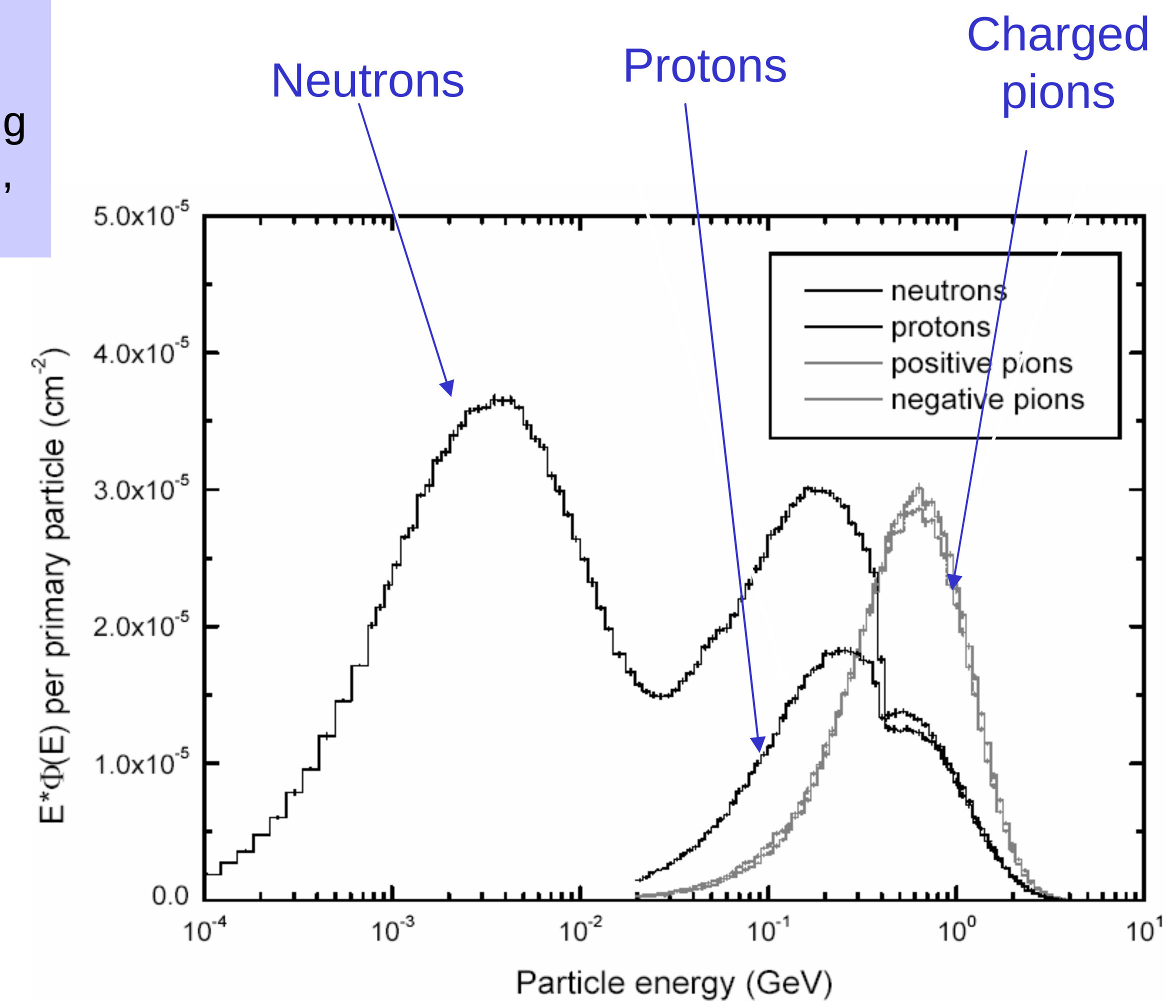

S. Agosteo, E. Dimovasili, A. Fassò and M. Silari, Radiat. Prot. Dosim. 110, 161-168, 2004

BSS response to charged hadrons

The problem is mostly with the lead-loaded spheres

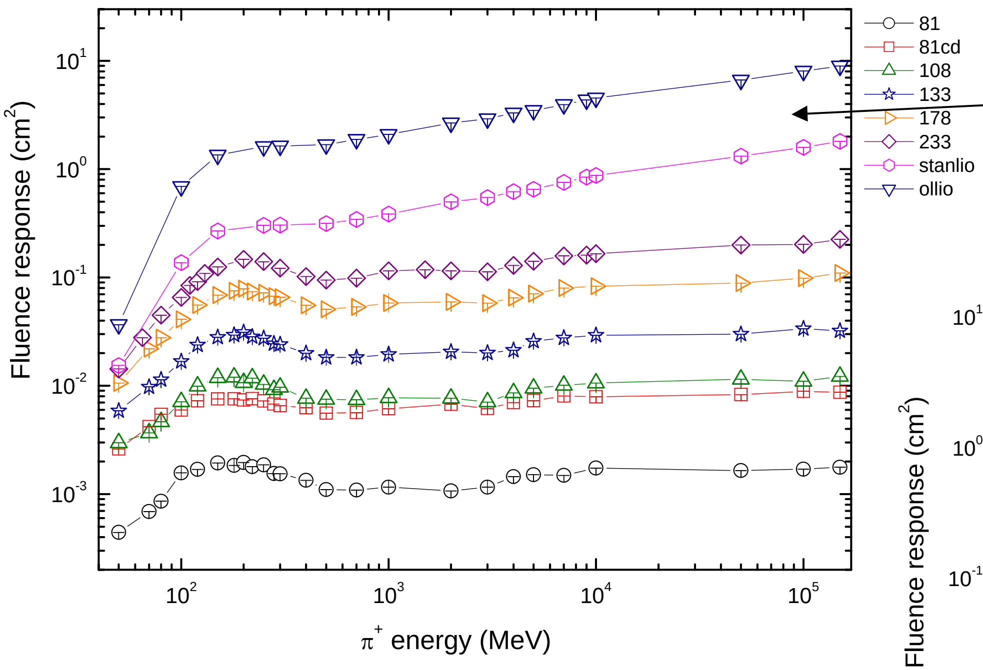

Positive pions

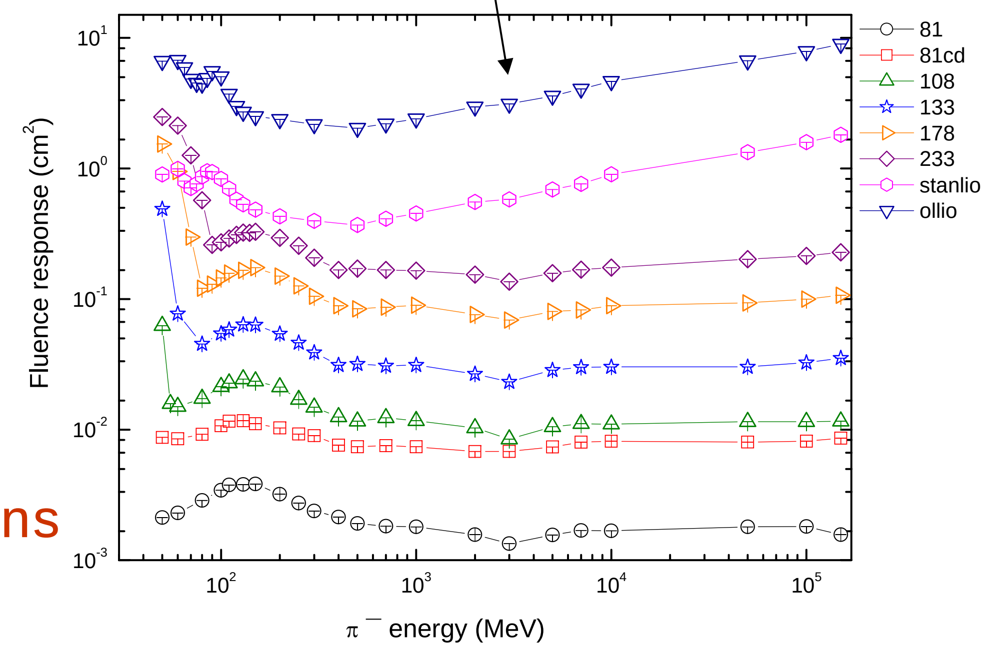

Negative pions

S. Agosteo, E. Dimovasili, A. Fassò and M. Silari, Radiat. Prot. Dosim. 110, 161-168, 2004

A Tissue Equivalent Proportional Counter (TEPC) is a proportional counter constituted by a tissue-equivalent gas contained in a cavity inside walls of a TE plastic. Acting on the gas pressure it is possible to simulate the events of energy deposition in microscopic volumes

The energy deposition in the TE gas is measured through ionization of primary charged particles and/or secondary particles generated mainly in the walls of the detector

It measures the probability distribution of absorbed dose d(y) in terms of lineal energy y (the ratio of energy imparted to matter in a volume by a single deposition event to the mean chord length in that volume)

From the probability distribution of absorbed dose d(y) one can evaluate the dose equivalent through a function Q(y) which relates the quality factor to the lineal energy

HAWK-TEPC
Tissue Equivalent Proportional Counter

Peter Beck and Sofia Rollet, Health Physics Division
ARC Seibersdorf research, Austria

Credit: ARC Seibersdorf research

TEPC - Tissue Equivalent Proportional Counter

- Absorbed Dose (Gy), Q(LET), Dose Equivalent (Sv)
- 1-2 µm tissue volume
- Microdosimetric spectra (y/kev μm^{-1})
- Measurements:
  - Photons: up to 7 Mev
  - Neutrons: up to 200 MeV
  - Mixed radiation field (CERF)
  - Heavy Ions

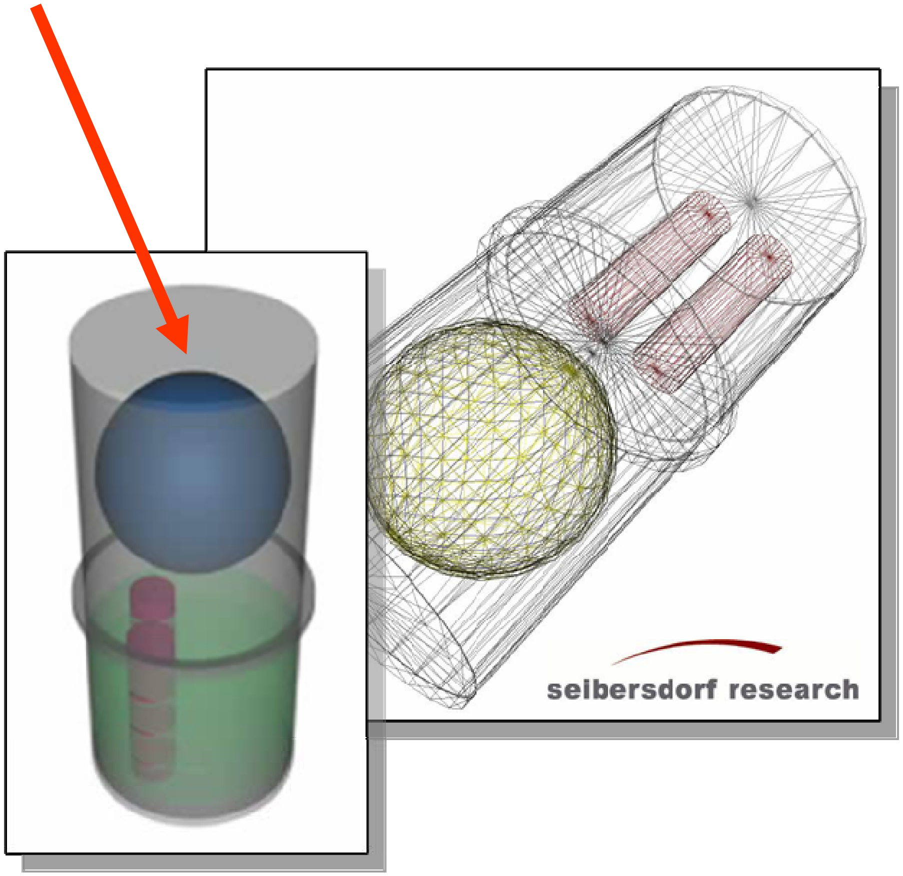

Credit: ARC Seibersdorf research

TEPC Absorbed Dose Measurements and FLUKA Simulation CERF facility for mixed Radiation Field

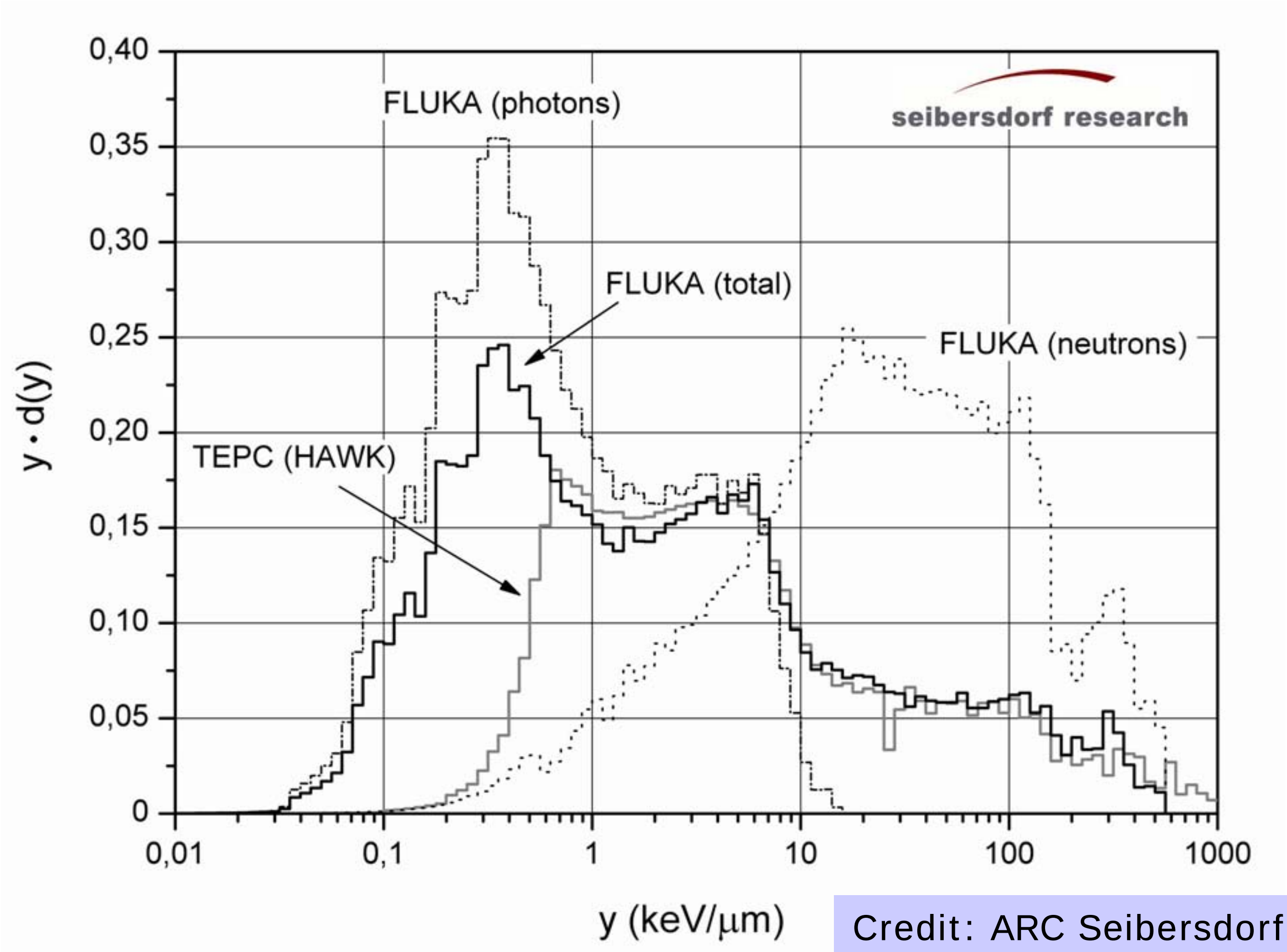

Credit: ARC Seibersdorf research

TEPC Absorbed Dose Measurements and FLUKA Simulation CERF facility for mixed Radiation Field

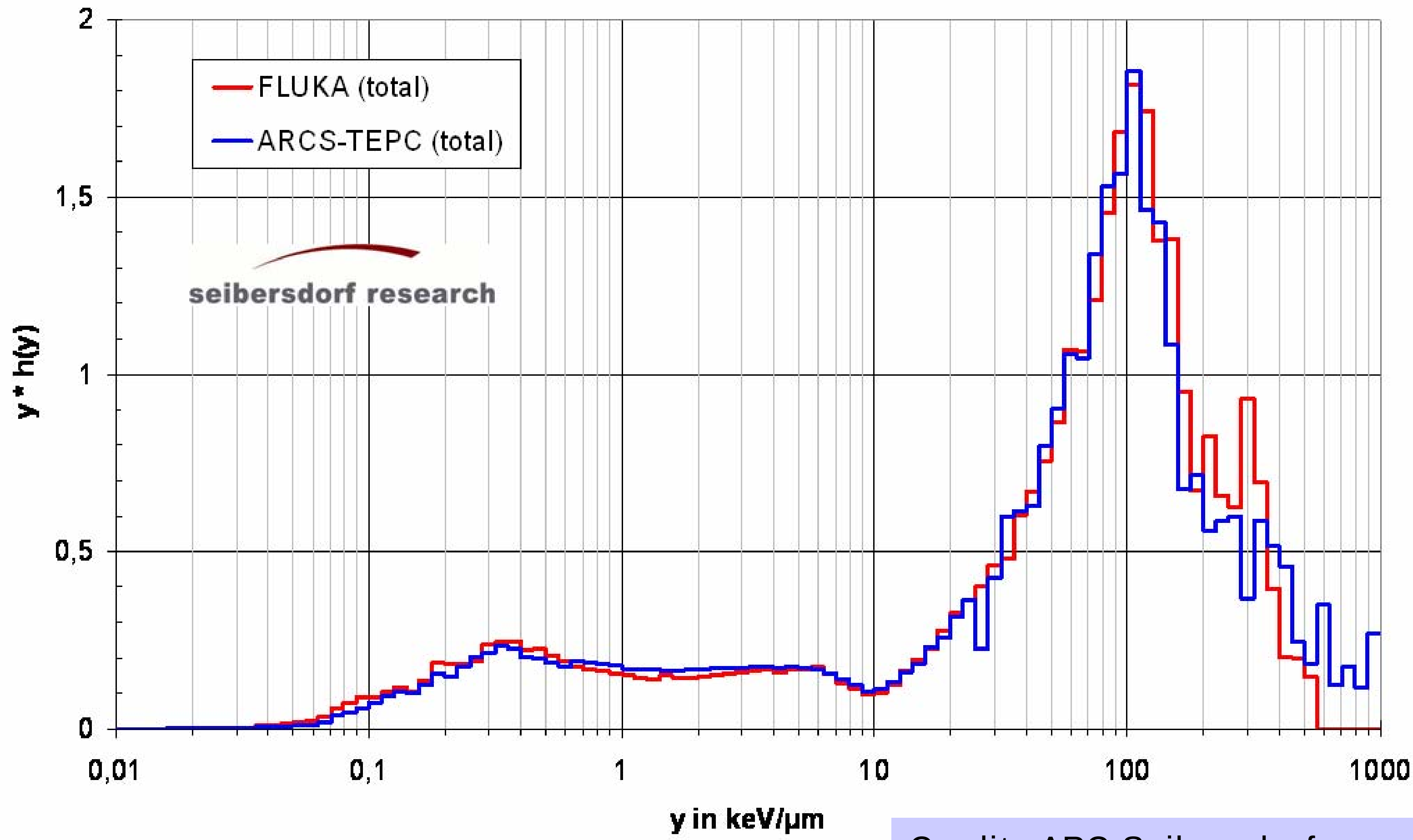

Credit: ARC Seibersdorf research

TEPC Simulation by FLUKA
Microdosimetric Spectra in Cosmic Radiation Field

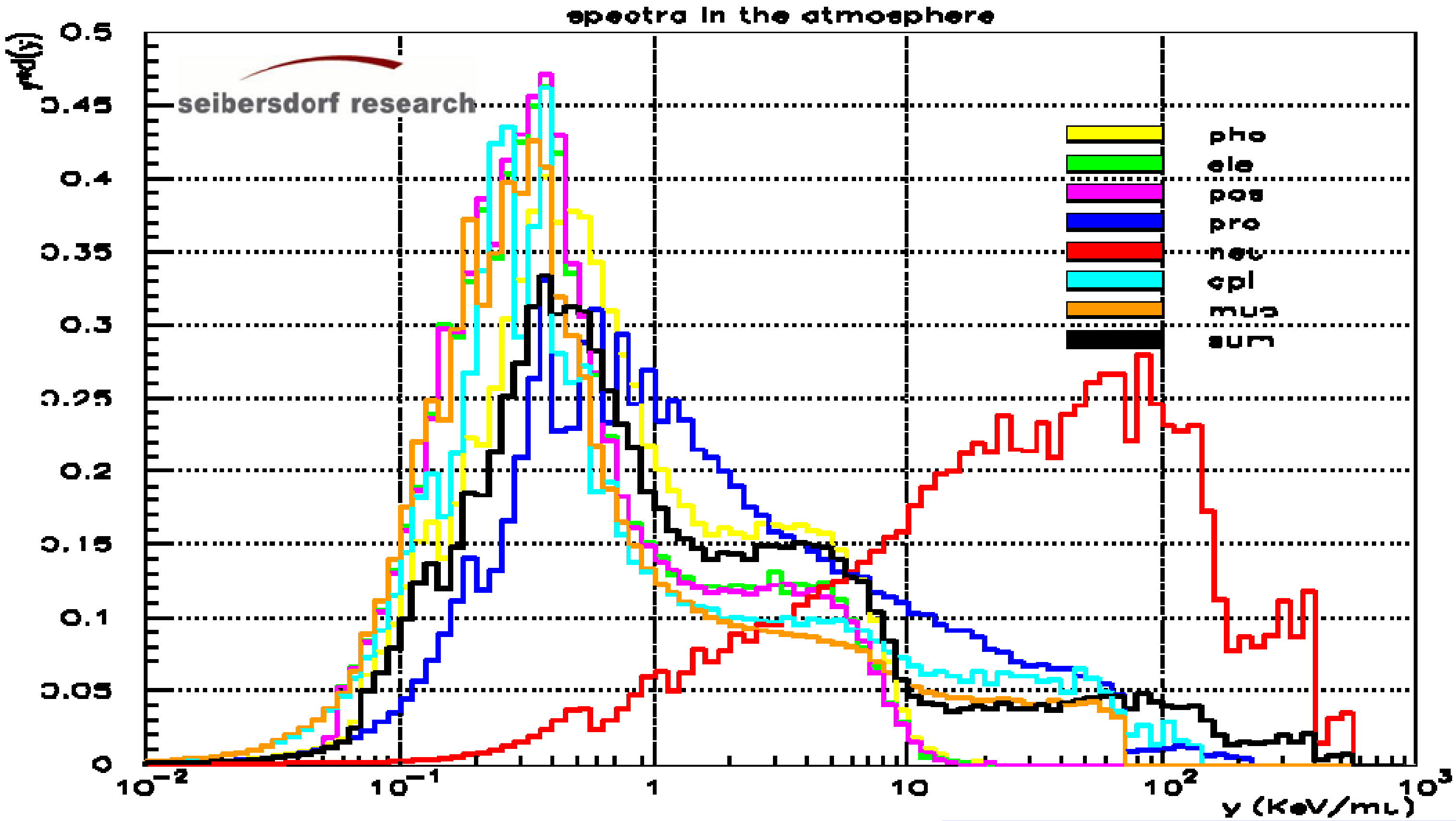

Credit: ARC Seibersdorf research

FLUKA Heavy Ion Simulation in TEPC
Oxygen 400 MeV/u, Beam Size: 8 x 8 cm^2

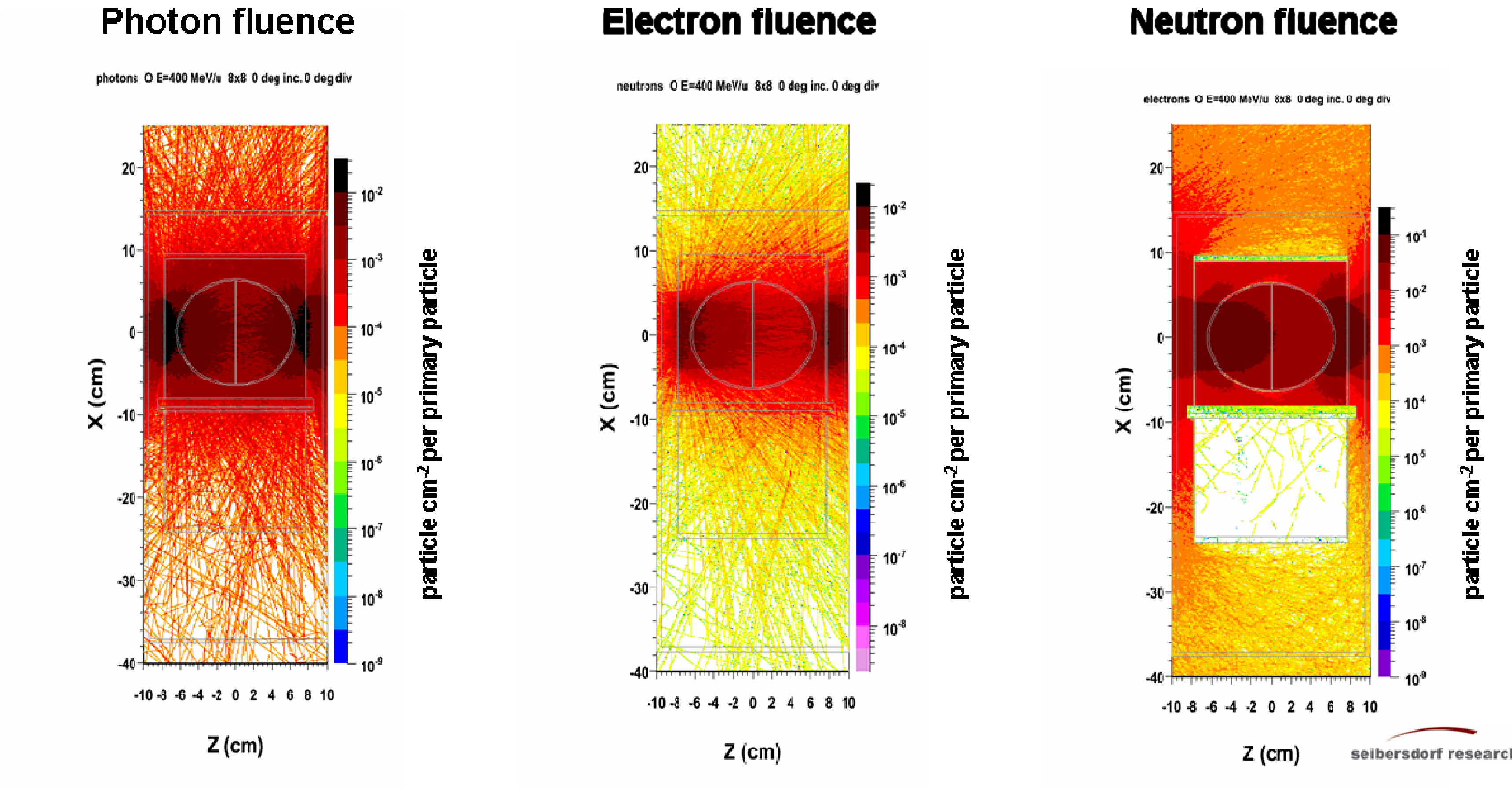

Credit: ARC Seibersdorf research

George Xu - Consortium of Computational Human Phantoms (CCHP) http://www.virtualphantoms.org/

Different groups from Germany, UK, USA, Japan, Korea and Brazil

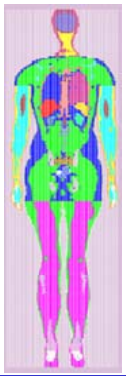
Golem/ICRP

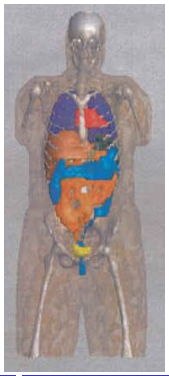
Helga


Irene


Donna

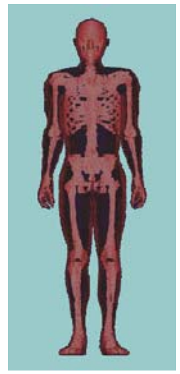
NORMAN

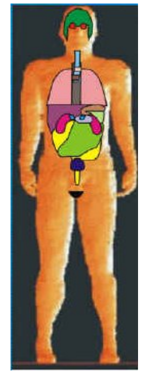
MAX

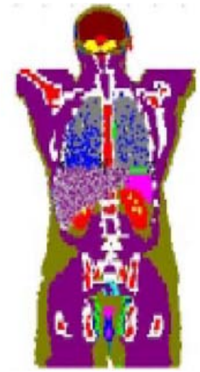
Zubal's

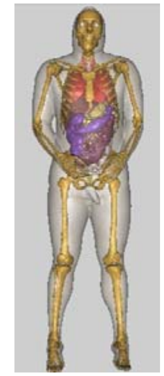
VIP-MAN


Otoko

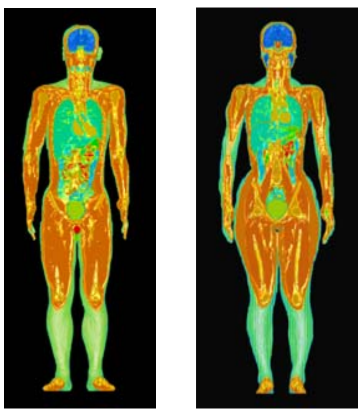
Nagaoka

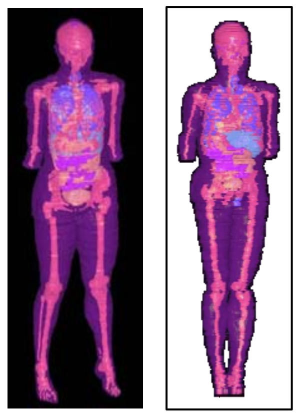
KORMAN

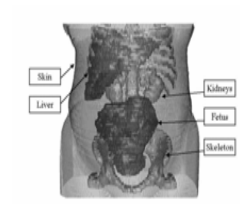

Mother/Fetus


UF-Newborn


UF-Newborn

Courtesy B. Kirk, ORNL

Specificity of an irradiation accident

- Type of irradiation: *total body or localised*
- Parameters of the source: *activity, type and energy of the radiation, duration of the exposure*
  ⇨ *attenuation in tissue, absorbed dose*
- The dose is an indicator of the effects expected in a tissue or organ allowing clinicians to
  - establish a diagnosis
  - decide a treatment
- The objective is to determine the dose and its distribution in the body

How to evaluate the dose?

- **Clinical data :** *symptoms (erythema...)*
- **Biological dosimetry :** *bio-indicators (chromosome aberrations...)*
- **Physical dosimetry :** *measurements and simulations*
    - Dosimetric evaluation of the dose via experimental methods
    - Dosimetric evaluation of the dose via numerical methods
    - Dose measurements on materials irradiated during the accident

Accident in Chile, December 2005

Place: construction site of a manufactory plant for the fabrication of cellulose

Context: source employed for industrial radiography welding controls found outside its shielded container

Characteristics of the source:
iridium-192, 3.3 10^{12} Bq (90 Ci)

Irradiation details:
- duration of exposure: *40 min, including 10 min in the rear pocket of the person trousers*
- suspected localised irradiation: *buttock, hands, head and chest*

source

Courtesy: J-F Bottolier-Depois, IRSN

Dosimetric reconstruction of the incident:
modelling the source in the pocket

Scanner

Voxel phantom

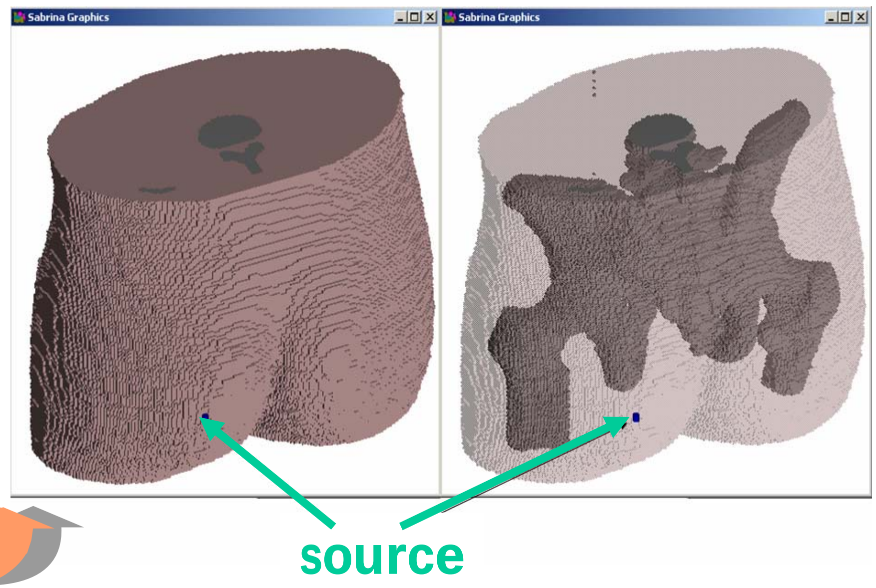

Monte Carlo

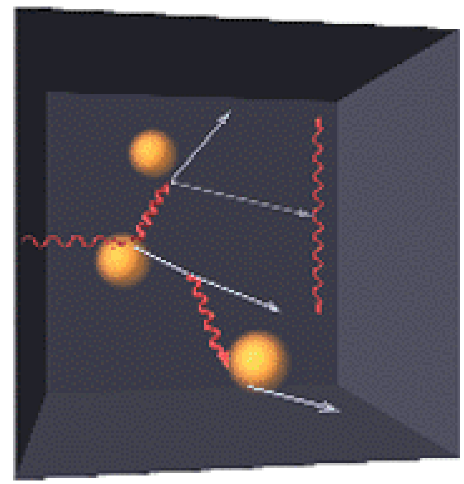

Courtesy: J-F Bottolier-Depois, IRSN

Monte Carlo calculations:

- Transport of the source photons in matter
- Energy deposition in various tissues and organs of the body

Dose distribution:
source in the rear pocket of trousers for 10 minutes

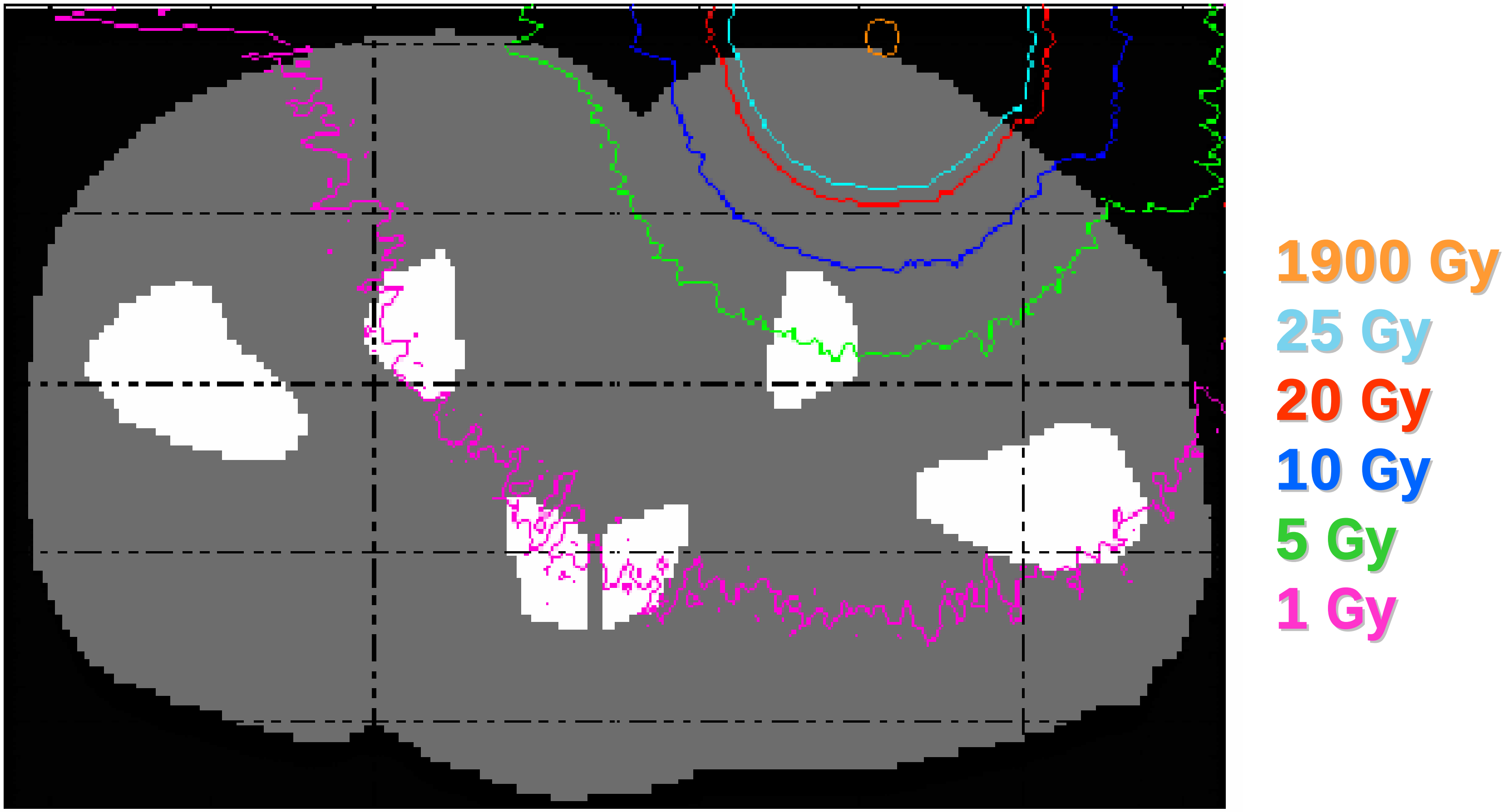

Above 25 Gy → tissue necrosis

Courtesy: J-F Bottolier-Depois, IRSN

Dose map as a direct support to surgery: *a world première*

Late intervention: *surgery is generally guided by the clinical picture since necrosis is evident*

Early intervention (the present case): *surgery is extended to potentially necrotic tissues, even if they look healthy at the moment surgery is decided*

A new approach: *the dose map on the surface and at depth drives the surgery*

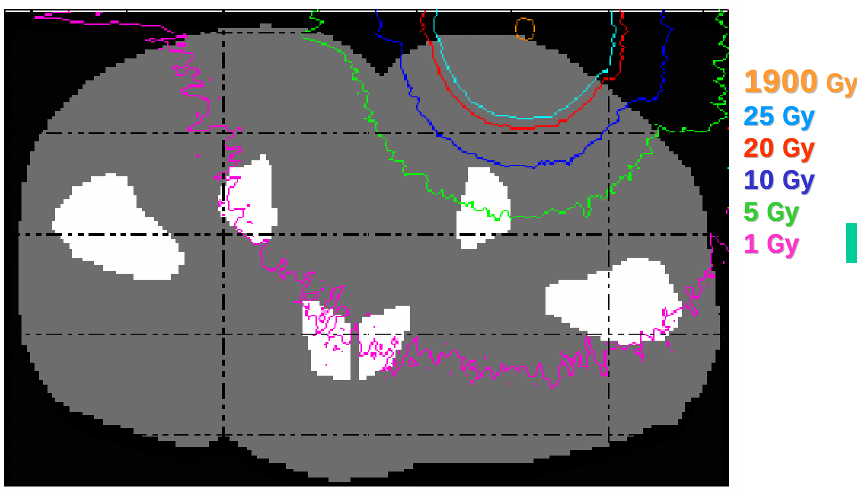

Dose distribution

5 cm

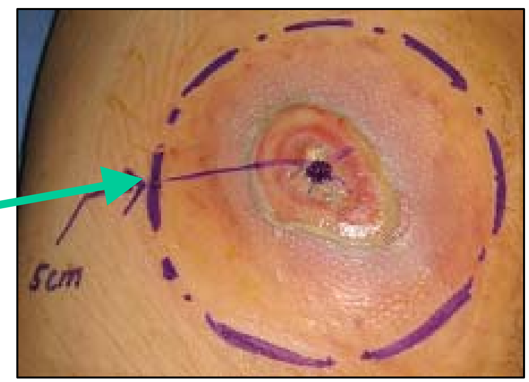

Surgery

Courtesy: J-F Bottolier-Depois, IRSN

Accident in Belgium, March 2006

Place: Industrial sterilisation plant

Installation GAMMIR II :
- cobalt-60, 2.96 10^{16} Bq (800,000 Ci)
- dose rate ~ 5000 Gy/h
- « plane » source: h 1.8 m - l 1 m, stored in a pool 6 m depth

Suspected irradiation: detected by doctor following blood test of worker showing a medullary aplasie, indicating acute irradiation

Circumstances of the accident: malfunctioning of the source control system, which caused the source to leave its shielded location unexpectedly

Courtesy: J-F Bottolier-Depois, IRSN

Irradiation details:
- duration of the exposure: 20 s
- total body irradiation with acute irradiation syndrome

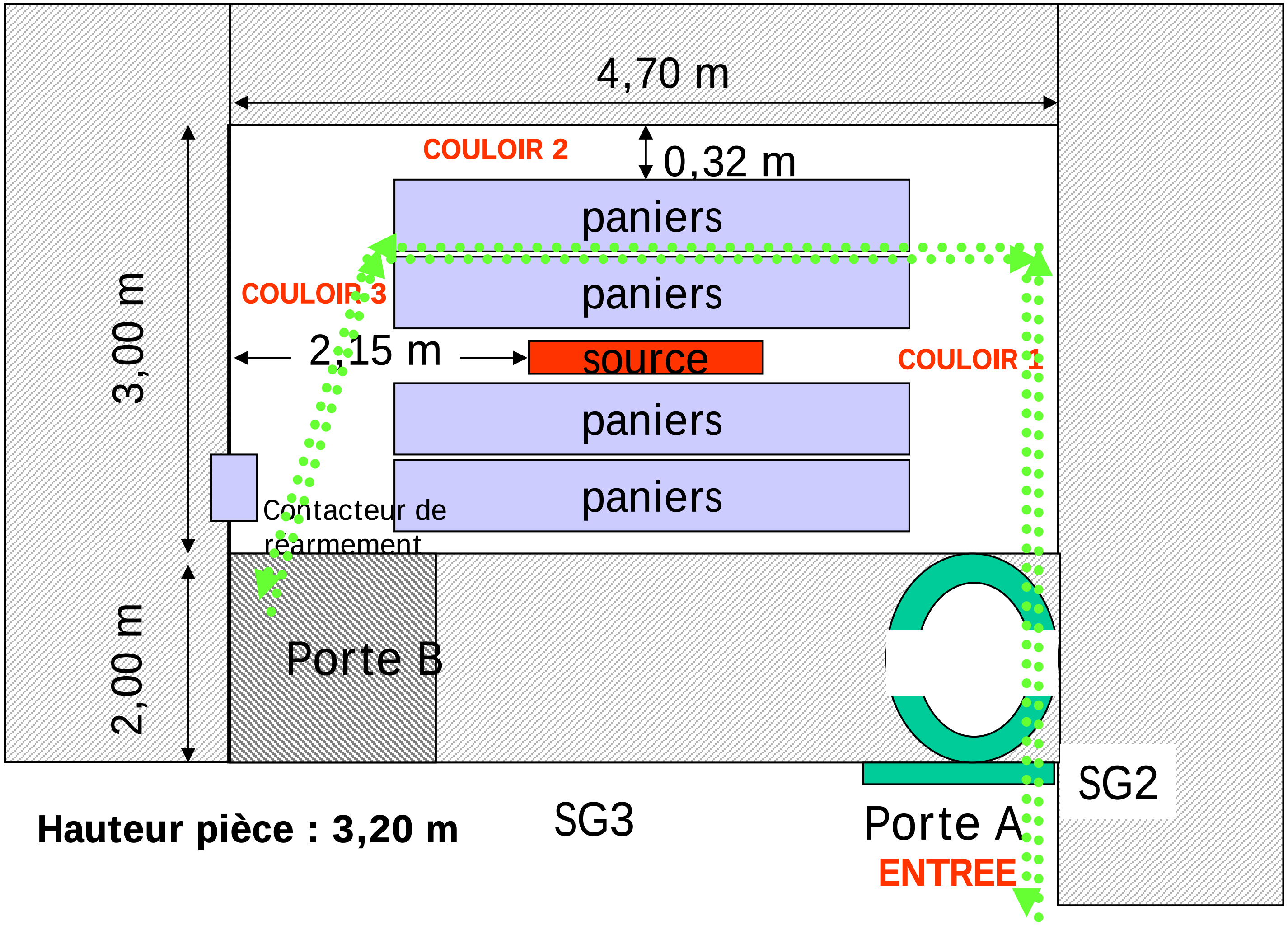

Hauteur pièce : 3,20 m

Courtesy: J-F Bottolier-Depois, IRSN

Evaluation of dose gradient within the body:
to assess whether a spontaneous recover of the bone marrow activity can be expected

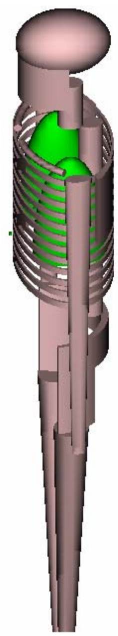

Voxel phantom

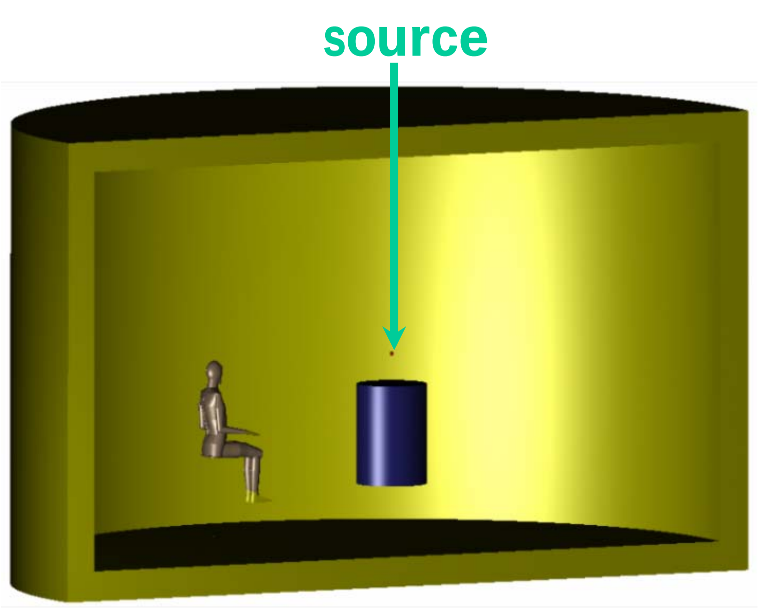

Environment:
position of irradiated person, room configuration, shielding…

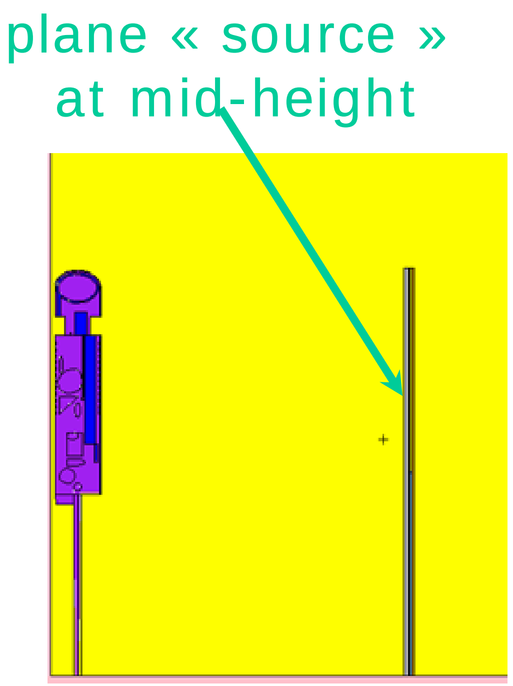

Courtesy: J-F Bottolier-Depois, IRSN

Calculation of the dose received by bone marrow tissues

Front view

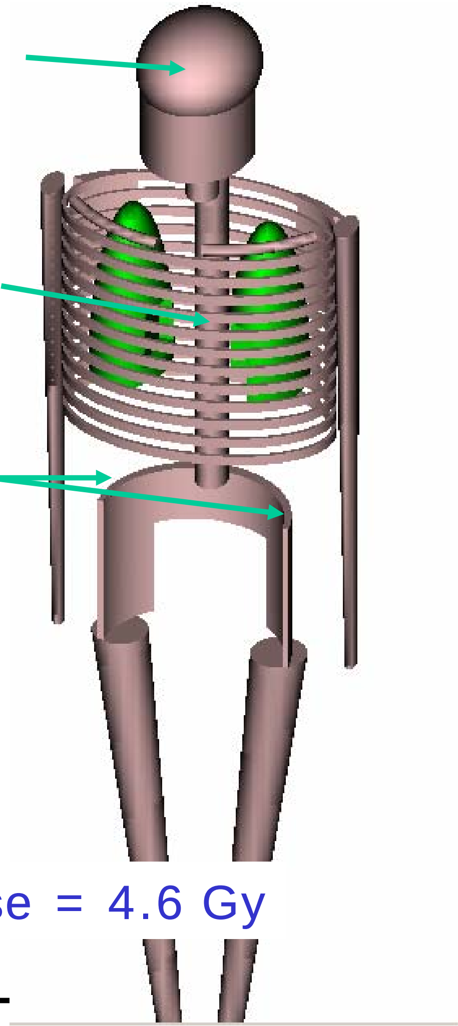

Skull : **1.5 Gy**

Sternum : **2.3 Gy**

Iliac crests : **3.4 Gy**

Back view

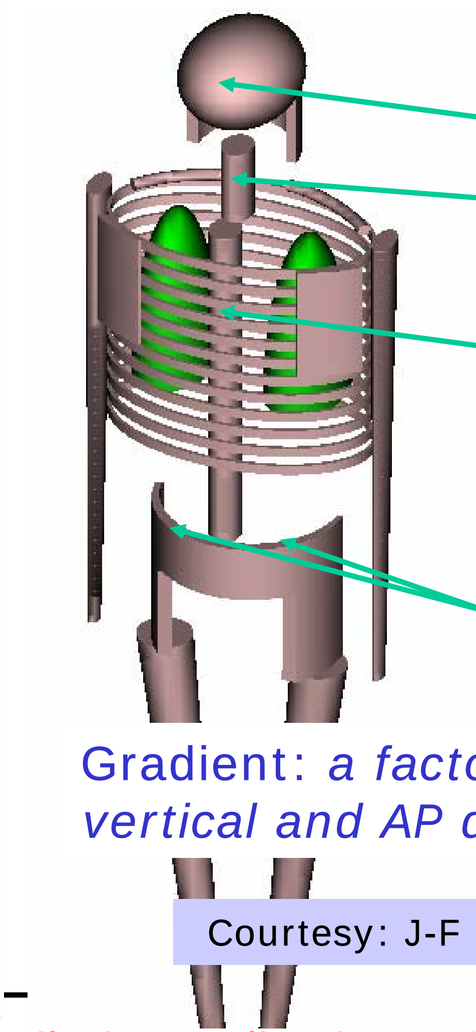

Skull: **3.3 Gy**

Cervicales : **3.3 Gy**

Spine : **4.8 Gy**

Iliac crests : **6.4 Gy**

Gradient: *a factor of 2 in the vertical and AP directions*

Average body dose = 4.6 Gy

Courtesy: J-F Bottolier-Depois, IRSN

The role of neutrons in Hiroshima and Nagasaki on cancer risk estimates from the A-bomb survivors

W. Rühm, L. Walsh, A.M. Kellerer
Institute for Radiation Protection, GSF Research Center for Environment and Health

The A-bomb explosions over

Hiroshima	Nagasaki

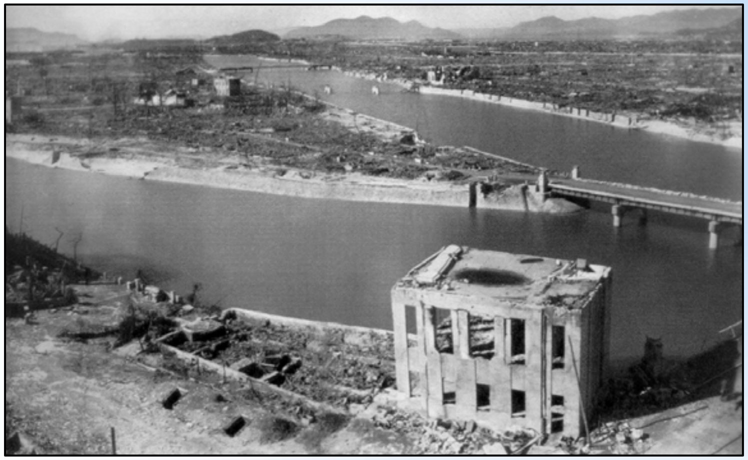

- August 6th 1945, 8:15
- inhabitants: 350,000
- deaths (end of 1945): 140,000

- August 9th 1945, 11:02
- inhabitants: 270,000
- deaths (end of 1945): 70,000

Study of Radiation-induced *Late* Effects among the A-bomb Survivors

Principle (simplified)

e.g. solid cancers, leukaemia
as a function of age, sex, organ, …

Done by the Radiation Effects Research Foundation (RERF) in Hiroshima and Nagasaki

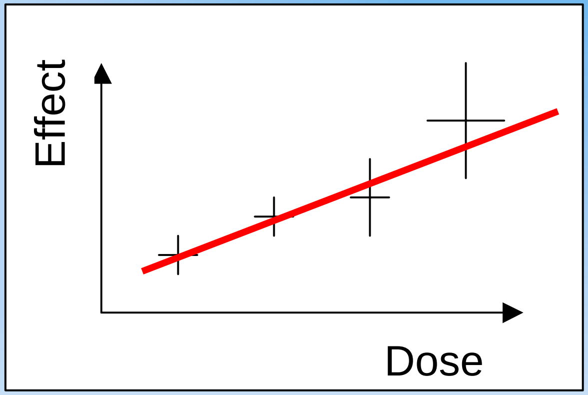

> effect per dose
> basis for risk estimates used by ICRP

y-axis:	x-axis:
Life Span Study (LSS)	**Dosimetry System 2002** (DS86)

Survivor location at the time of bombing, Hiroshima

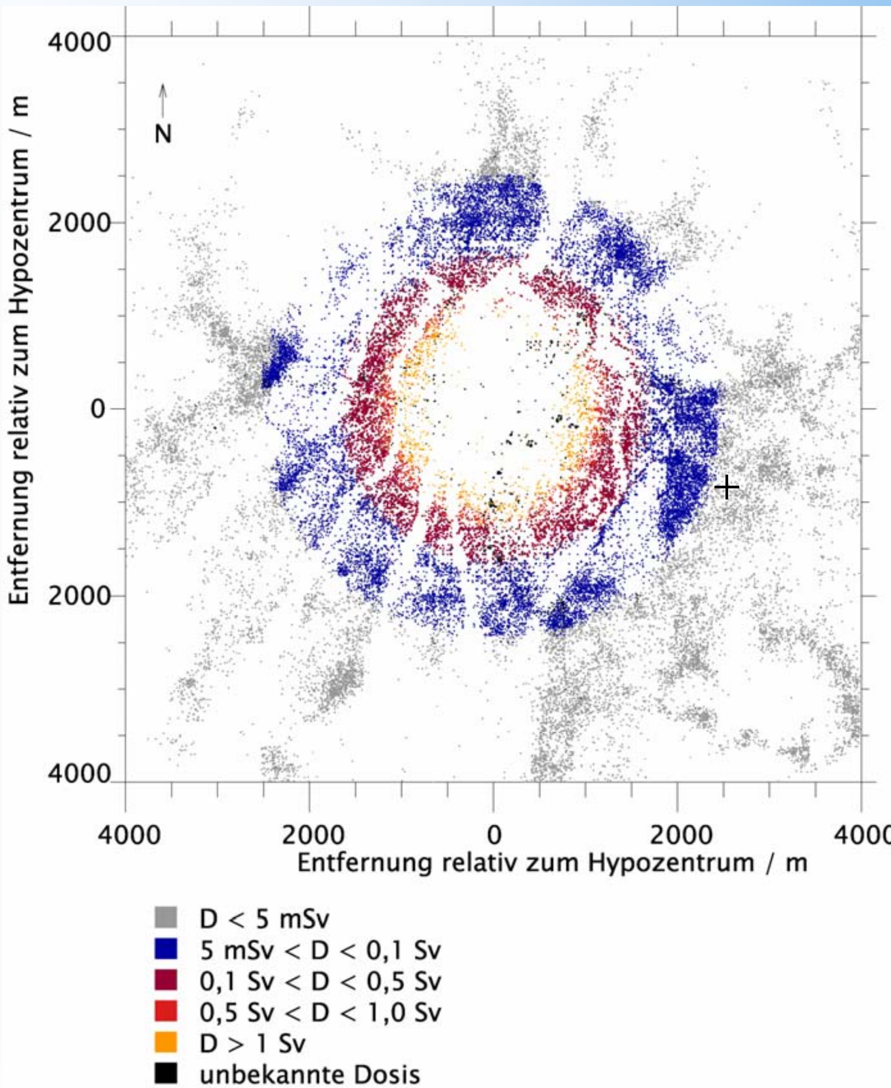

Picture produced by M. Chomentowski (Radiobiological Institute, LMU Muich, Germany), during a visit of the Radiation Effects Research Foundation, Hiroshima, Japan

The Dosimetry Systems DS86/DS02

Principle: Coupled neutron-gamma transport calculations from epicentre to target organ

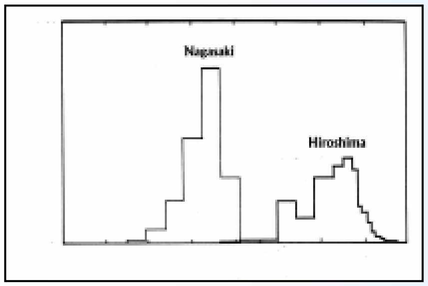

Neutron source terms

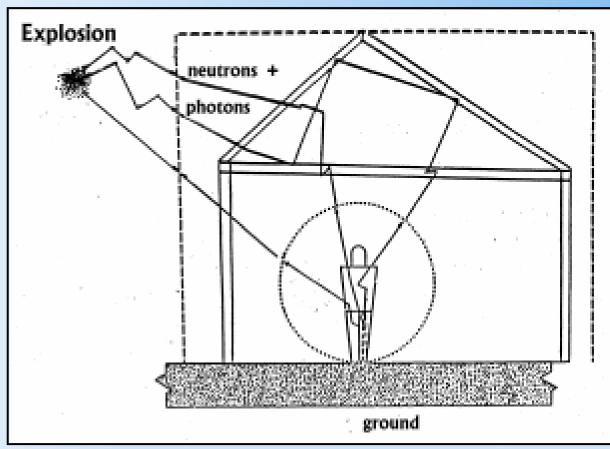

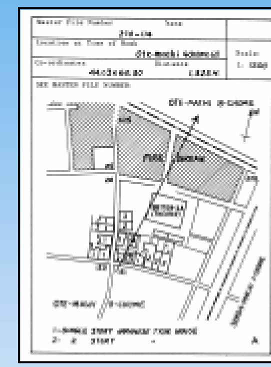

Individual location

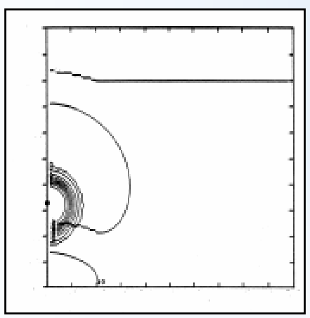

Iso-contours of air density

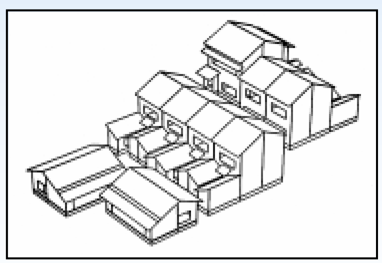

House cluster

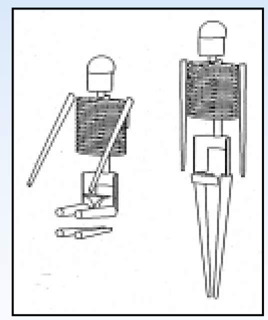

Human phantoms

Pictures taken from:
W.C. Roesch (ed.). US-Japan joint Reassessment of Atomic Bomb Radiation Dosimetry in Hiroshma snd Nagasaki, Final report, RERF, Hiroshima, Japan

G s - Persdos

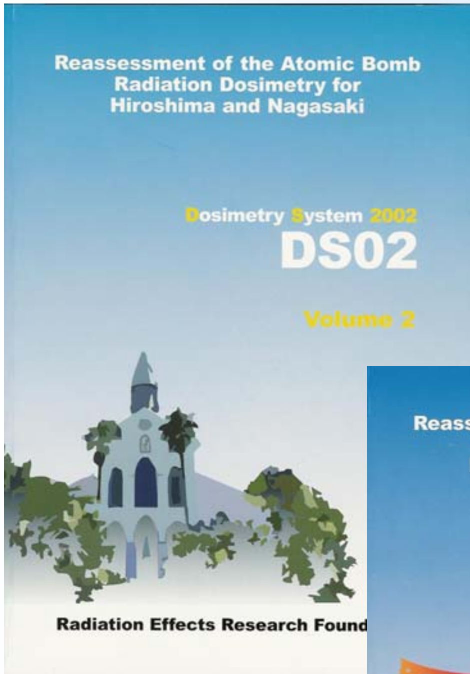

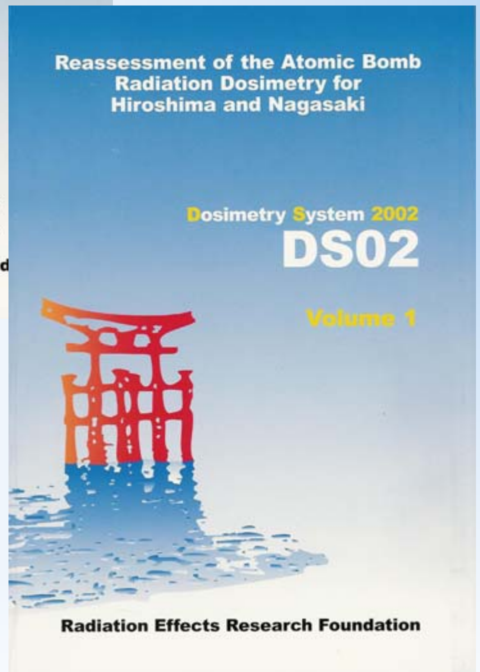

since 02/06

www.rerf.or.jp

T. Straume, G. Rugel, A.A. Marchetti, W. Rühm, G. Korschinek, J.E. McAninch, K.L. Caroll, S. Egbert, T. Faestermann, K. Knie, R.E. Martinelli, A. Wallner, C. Wallner. Measurement of ^{63}Ni in copper samples from Hiroshima and Nagasaki by AMS.

W. Rühm, G. Rugel, T. Faestermann, K. Knie, A. Wallner, B. Heisinger, E. Nolte, A.A. Marchetti, R.E. Martinelli, K.L. Carroll, G. Korschinek. Evaluation of Cosmic-ray Induced ^{63}Ni Background in copper.

W. Rühm, T. Huber, E. Nolte, K. Kato, S.D. Egbert. Accelerator Mass Spectrometry Measurements of ^{36}Cl in Germany.

E. Nolte, T. Huber, W. Rühm, K. Kato, V. Lazarev, L. Schultz. Evaluation of Natural In-situ Production of ^{36}Cl in Mineral Samples.

M. Hoshi, S. Endo, M. Ishikawa, T. Straume, K. Komura, W. Rühm, T. Huber, E. Nolte, Y. Nagashima, H. Fukushima, T. Imanaka. Intercomparison Study for ^{152}Eu and ^{36}Cl Measurements.

W. Rühm, T. Huber, K. Kato, E. Nolte, T. Imanaka, S. Egbert. Trace Element Concentrations in Granite and their Impact on Thermal Neutron Activation.